

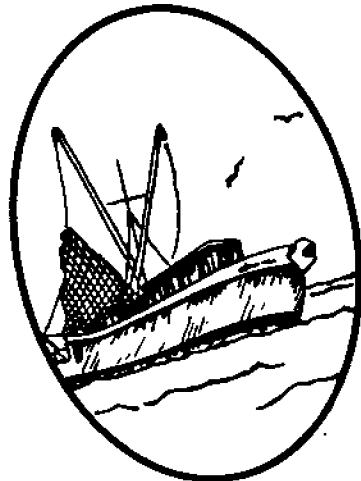
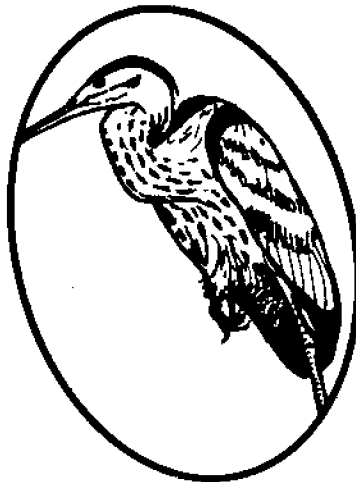
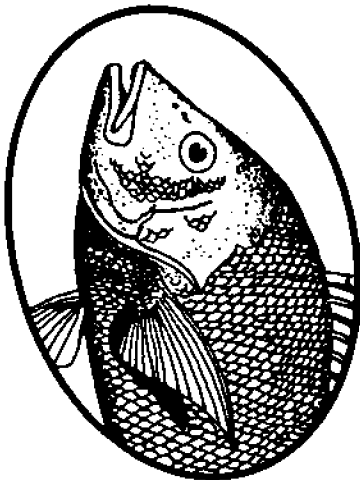
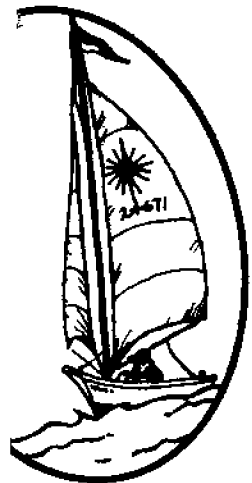
CIRCULATING COPY  
Sea Grant Depository

LOAN COPY ONLY

Working Paper 84-2

# Evaluation of the Extent Of Hurricane-Induced Flooding On Coastal Urban Areas in North Carolina

T.C. Gopalakrishnan, C.C. Tung, and J.S. Wei



NATIONAL SEA GRANT DEPOSITORY  
PELL LIBRARY BUILDING  
URI, NARRAGANSETT BAY CAMPUS  
NARRAGANSETT, RI 02882

UNC Sea Grant College Program  
105 1911 Building  
North Carolina State University  
Raleigh, NC 27650

**CIRCULATING COPY**  
**Sea Grant Depository**

EVALUATION OF THE EXTENT OF HURRICANE-INDUCED  
FLOODING ON COASTAL URBAN AREAS IN NORTH CAROLINA

By

T. C. Gopalakrishnan

C. C. Tung

J. S. Wei

Department of Marine, Earth and Atmospheric Sciences

and

Department of Civil Engineering

North Carolina State University

Raleigh, North Carolina 27650

This work was sponsored by the Office of Sea Grant, NOAA, U.S. Department of Commerce, under Grant No. R/CZS-18 and the North Carolina Department of Administration. The U.S. Government is authorized to produce and distribute reprints for governmental purposes notwithstanding any copyright that may appear hereon.

UNC Sea Grant College Publication UNC-SG-WP-84-2

September, 1983

\$2.50

NATIONAL SEA GRANT DEPOSITORY  
PELL LIBRARY BUILDING  
URI, NARRAGANSETT BAY CAMPUS  
NARRAGANSETT, RI 02882

## ABSTRACT

This study is concerned with the problem of flooding due to storm and wave surge for the coast of North Carolina using a numerical finite element method.

In the interest of saving computational time, a combination of one-dimensional and two-dimensional finite element models is used. That is, in the offshore region, storm surge is evaluated using a two-dimensional model. Near-shore and on land, storm surge and wave surge are computed using a one-dimensional model. A salient feature of the one-dimensional model is its ability to handle moving boundaries and to compute intrusion distance after the waves break and the surge floods the land.

The finite element method is applied to six sections of the North Carolina coast using the 1954 Hurricane Hazel as the forcing storm.

## TABLE OF CONTENTS

LIST OF FIGURES . . . . .	ii
LIST OF TABLES . . . . .	iii
1. INTRODUCTION . . . . .	1
1.1 Numerical Finite Element Model . . . . .	1
1.2 Specific Tasks . . . . .	2
2. TWO-DIMENSIONAL MODEL FOR OFFSHORE REGION . . . . .	3
2.1 The Hydrodynamic Equations . . . . .	3
2.2 The Hurricane Model . . . . .	4
3. ONE-DIMENSIONAL MODELS FOR NEAR-SHORE REGION . . . . .	5
3.1 Propagation of Waves . . . . .	5
3.2 Numerical Technique . . . . .	6
3.2.1 Finite element discretization . . . . .	7
3.2.2 Time dependent front element . . . . .	7
3.2.3 Wave breaking . . . . .	9
3.2.4 Boundary and initial conditions . . . . .	10
3.3 Movement of Storm Surge on Land . . . . .	10
4. DATA COLLECTION . . . . .	11
4.1 Hurricane Data . . . . .	12
4.2 Offshore and Near-shore Profiles . . . . .	12
4.3 Tidal Variation . . . . .	13
4.4 Wave Heights . . . . .	13
4.5 Longshore Current . . . . .	14
4.6 Storm Surge . . . . .	14
4.7 Flooding Extent . . . . .	14
5. COMPUTATIONS . . . . .	14
5.1 Storm Surge Offshore . . . . .	14
5.2 Storm Surge and Wave Run-up . . . . .	15
6. VALIDATION . . . . .	15
6.1 Comparison with Experiment . . . . .	15
6.2 Comparison with Field Observations . . . . .	16
REFERENCES . . . . .	18
APPENDIX . . . . .	58
COMPUTER PROGRAM . . . . .	58

## LIST OF FIGURES

1.	Hurricane parameters . . . . .	22
2.	Near shore region . . . . .	23
3.	Spatial discretization . . . . .	24
4.	Water profile and end-element at time $t$ . . . . .	25
5.	Water profile and end-element at time $t + \Delta t$ . . . . .	25
6.	Position at time $t$ . . . . .	26
7.	Position at time $t + \Delta t$ . . . . .	26
8.	Element splitting at time $t + \Delta t$ . . . . .	27
9.	Downstream conditions at the instants $t$ and $t + \Delta t$ . . . . .	27
10.	Definition sketch (distorted scale model) . . . . .	28
11.	Actual and hypothetical paths of Hurricane Hazel . . . . .	29
12.	Region 1: Brown Inlet . . . . .	30
13.	Region 2: Kure Beach . . . . .	31
14.	Region 3: Wilmington Beach . . . . .	32
15.	Region 4: Roanoke Island . . . . .	33
16.	Region 5: Hampstead . . . . .	34
17.	Region 6: Cape Fear . . . . .	35
18.	(a) Bottom profile near Brown Inlet . . . . .	36
18.	(b) Bottom profile near Kure Beach . . . . .	36
18.	(c) Bottom profile near Wilmington . . . . .	37
18.	(d) Bottom profile near Roanoke Island . . . . .	37
18.	(e) Bottom profile near Hampstead . . . . .	38
18.	(f) Bottom profile near Cape Fear . . . . .	38
19.	Time history of tide range - NC coast sample . . . . .	39
20.	Hurricane paths and tide heights . . . . .	40
21.	Offshore region east of Cape Hatteras . . . . .	41
22.	Discretization of the region east of Cape Hatteras . . . . .	42
23.	Offshore region south of Cape Hatteras . . . . .	43
24.	Discretization of the region south of Cape Hatteras . . . . .	44
25.	(a) Storm tide - HZ0 - Ocracoke . . . . .	45
25.	(b) Storm tide - HZ0 - Cape Hatteras . . . . .	46
25.	(c) Storm tide - HZ0 - Nags Head . . . . .	47
26.	(a) Storm tide - HZ1 - Ocracoke . . . . .	48
26.	(b) Storm tide - HZ1 - Cape Hatteras . . . . .	49
26.	(c) Storm tide - HZ1 - Nags Head . . . . .	50
27.	(a) Storm tide - HZ2 - Ocracoke . . . . .	51
27.	(b) Storm tide - HZ2 - Cape Hatteras . . . . .	52
27.	(c) Storm tide - HZ2 - Nags Head . . . . .	53
28.	(a) Storm tide - HZ3 - Ocracoke . . . . .	54
28.	(b) Storm tide - HZ3 - Cape Hatteras . . . . .	55
28.	(c) Storm tide - HZ3 - Nags Head . . . . .	56
29.	Experimental wave run-up (after Horikawa 1978) . . . . .	57

## LIST OF TABLES

1. Coefficients of polynomials representing bottom profiles of six sections . . . . . 20
2. Intrusion distance for the six sections . . . . . 21

## EVALUATION OF THE EXTENT OF HURRICANE-INDUCED FLOODING ON COASTAL URBAN AREAS IN NORTH CAROLINA

### 1. INTRODUCTION

Coastal areas of North Carolina have been visited frequently by severe tropical storms. A Civil Defense report (Griffin 1955) indicates that in the period between 1879 and 1955, there were as many as 270 storms of hurricane intensity in the Caribbean and Atlantic areas. Recently, within a period of one year (from 1954 to 1955) North Carolina was struck by four hurricanes each of which caused great damage to life and property.

Several administrative measures were taken by the state government after 1955 in order to prevent and investigate storm damage. In tune with this move, the Sea Grant Program has funded several projects related to the analysis and prediction of wind-generated waves on the coast of North Carolina. The present project under the Sea Grant Program is intended to develop a numerical tool for the prediction of the extent of flooding due to storm surge.

Since the development of the numerical finite element computer program constitutes a major part of the present study, a brief discussion of related past work and the special features of the present model are first given.

#### 1.1 Numerical Finite Element Model

The equations governing storm surge are nonlinear. Therefore, we must resort to numerical solutions. The method of finite difference has been used by many investigators. Among these investigators, we mention Reid and Bodine (1968), Jelesnianski (1967, 1974, 1976), Pearce (1972), Damsgaard and Dinsmore (1975), and Wanstrath (1977). More recently, Tetra Tech, Inc. (1981) published a report on coastal flooding analysis using the finite difference method. The use of the finite element method for fluid flow problems is relatively new. Wang and Connor (1975) used the finite element method to study ocean circulation. This approach was adopted by Chen (1978) for the computation of storm surge at the Chesapeake Bay-ocean system. The finite element method used in the present study follows that of Wang and Connor (1975) and Chen (1978). Emphasis in this present study is placed on the development of special techniques for the treatment of over-land motion of storm surge and storm waves riding on surge. Some past studies have followed over-land motion through a set of discrete jumps (Tetra Tech 1981, Yeh and Chou 1979). However, those studies did not include the effects of waves riding on the storm surge. In the present study, we take into account the presence of storm waves and follow the moving boundary of water continuously instead of in discrete jumps.

To save computational time, we divide the coastal region into two parts. In the offshore region, storm surge is evaluated using a two-dimensional model. Near-shore and on land, storm surge and wave surge are computed using one-dimensional models.

## 1.2 Specific Tasks

The specific tasks undertaken in this study are stated in the following:

1. Development of numerical finite element models for the computation of storm surge offshore, and storm surge and wave run-up near-shore and on land.
2. Collection of data to provide input to the models and for validation purpose. The data include characteristics of Hurricane Hazel, offshore and near-shore bottom profiles, tidal variation, storm wave characteristics, long-shore currents, storm and wave surge and flooding extent for the coast of North Carolina.
3. Application of the numerical models to six selected sections in North Carolina using Hurricane Hazel as the forcing storm to assess flooding extent and compare it with observations.

Discussion of the methodology underlying the development of the finite element models and the special features introduced in the treatment of surge and wave run-up are contained in Sections 2 and 3. Description of the data collected is given in Section 4. In Section 5, the numerical results obtained are presented and validation of these results is given in Section 6.



## 2. TWO-DIMENSIONAL MODEL FOR OFFSHORE REGION

### 2.1 The Hydrodynamic Equations

The hydrodynamic equations used are the vertically integrated momentum and mass conservation equations. Namely

$$\frac{\partial H}{\partial t} + \frac{\partial q_x}{\partial x} + \frac{\partial q_y}{\partial y} = Q \quad (1)$$

$$\begin{aligned} \frac{\partial q_x}{\partial t} + \frac{\partial}{\partial x} \left( \frac{q_x^2}{H} \right) + \frac{\partial}{\partial y} \left( \frac{q_x q_y}{H} \right) - f_{\Omega} q_y &= -\frac{H}{\rho} \frac{\partial}{\partial x} (p^S + \rho g \eta) \\ + \frac{\partial T_{xx}}{\partial x} + \frac{\partial T_{xy}}{\partial y} + \frac{1}{\rho} (\tau_x^S - \tau_x^b) & \end{aligned} \quad (2)$$

$$\begin{aligned} \frac{\partial q_y}{\partial t} + \frac{\partial}{\partial x} \left( \frac{q_x q_y}{H} \right) + \frac{\partial}{\partial y} \left( \frac{q_y^2}{H} \right) - f_{\Omega} q_x &= -\frac{H}{\rho} \frac{\partial}{\partial y} (p^S + \rho g \eta) \\ + \frac{\partial T_{xy}}{\partial x} + \frac{\partial T_{yy}}{\partial y} + \frac{1}{\rho} (\tau_y^S - \tau_y^b) & \end{aligned} \quad (3)$$

Here,  $x$  and  $y$  denote the horizontal axes along the east and north directions, respectively,  $t$  is time,  $\eta(x,y,t)$  is water surface elevation above undisturbed water level,  $H(x,y,t) = h(x,y) + \eta(x,y,t)$ ,  $h(x,y)$  being undisturbed water depth,  $\rho$  is water density, and  $g$  is gravitational acceleration. The quantities

$$q_x(x,y,t) = \int_{-h}^{\eta} u(x,y,z,t) dz$$

$$q_y(x,y,t) = \int_{-h}^{\eta} v(x,y,z,t) dz$$

are water transport components in the  $x$  and  $y$  directions, respectively,  $u$  and  $v$  being the  $x$  and  $y$  components of water particle velocity,  $Q(x,y,t)$  is the rate of change of mass per unit area,  $f_{\Omega} = 2 \Omega \sin \phi$  is the Coriolis parameter,  $\Omega$  being the angular speed of earth's rotation,  $\phi$  is the latitude,  $p^S$  is atmospheric pressure,  $T$  are internal stresses,  $\tau^S$  are wind stress components and  $\tau^b$  are bottom friction components.

## 2.2 The Hurricane Model

An idealized hurricane model can be represented by the central pressure depression  $\Delta p$ , the distance from hurricane center to the point of maximum winds  $R_m$ , and the forward speed  $V_f$  of the hurricane (see Fig. 1). The National Weather Service reports these parameters in characterizing a hurricane.

The central pressure depression is defined as

$$\Delta p = p_\infty - p_c \quad (4)$$

where  $p_\infty$  is the atmospheric pressure at the outer periphery of the hurricane and  $p_c$  is the pressure at the center. Pressure at any other part at a distance  $r$  from the center is given by

$$p = p_c + \Delta p \exp\left(-\frac{R_m}{r}\right) \quad (5)$$

The wind stress on water in the  $x$  and  $y$  directions are given by

$$\tau_x = C \rho_a U_{10} U_{10x} \quad (6)$$

$$\tau_y = C \rho_a U_{10} U_{10y} \quad (7)$$

where  $\rho_a$  is air density ( $\text{Kg/m}^3$ ),  $C$  is wind drag coefficient and is given by

$$C = \begin{cases} C_0 & U_{10} \leq U_{cr} \\ C_0 + C_1 \left(1 - \frac{U_{cr}}{U_{10}}\right) & U_{10} \geq U_{cr} \end{cases}$$

$C_0 = 0.0011$ ,  $C_1 = 0.0025$  are dimensionless constants and  $U_{cr} = 7.2$  m/sec. The quantities  $U_{10x}$  and  $U_{10y}$  are  $x$  and  $y$  components of  $U_{10}$ , the wind velocity at 10m above water level which is given by (Pagenkopf 1976, Pearce 1972)

$$U_{10} = \frac{1}{2} \left\{ - [C_r f_\Omega r + V_f \sin(\theta + \beta)] + \left[ [C_r f_\Omega r + V_f \sin(\theta + \beta)]^2 + C_r^2 \frac{4\Delta p}{\rho_a} \frac{R_m}{r} \exp\left(-\frac{R_m}{r}\right) \right]^{1/2} \right\} \quad (8)$$

where  $\Delta p$  is in mb,  $C_r$  is a dimensionless reduction factor for  $U_{10}$ ,  $\beta$  is deflection angle and  $\theta$  is the angle between forward velocity  $V_f$  and the position vector  $r$  (see Fig. 1). The values used in this study are  $C_r = 0.875$  and  $\beta = 25^\circ$ .

### 3. ONE-DIMENSIONAL MODELS FOR NEAR-SHORE REGION

In the interest of saving computation time, surge and wave motion in the near-shore region and on land are computed using one-dimensional models. The link between the two-dimensional model for the offshore region and the one-dimensional models for the near-shore region is brought about by using the storm surge computed from the two-dimensional model offshore as input to the one-dimensional models at Section 1 shown in Fig. 2. Furthermore, the propagations of surge and wave near-shore and on land are performed separately.

#### 3.1 Propagation of Waves

The flow is assumed to be inviscid and incompressible. The density of water and atmospheric pressure remain constant. The effects of wind, percolation, Coriolis and tide-generating forces are neglected. It is assumed that currents are not present, the forcing wave enters at still-water conditions and the bottom is assumed to impart frictional effects.

If bottom friction is neglected, the momentum equations are

$$\frac{\partial u}{\partial t} + u \frac{\partial u}{\partial x} + w \frac{\partial u}{\partial z} = - \frac{1}{\rho} \frac{\partial p}{\partial x} \quad (9)$$

$$\frac{\partial w}{\partial t} + u \frac{\partial w}{\partial x} + w \frac{\partial w}{\partial z} = - \frac{1}{\rho} \frac{\partial p}{\partial z} - g$$

where  $x$  and  $z$  are horizontal and vertical axes shown in Fig. 2,  $u$  and  $w$  are velocity components and  $p$  is pressure. We now assume that horizontal velocity is independent of  $z$ . This assumption is valid because the depth is small compared to the horizontal extent of the disturbance. An essential aspect in the present study is that wave run-up involves considerable vertical acceleration and hence the usual shallow-water approach of assuming hydrostatic pressure distribution is no longer adequate. The effect of vertical acceleration is introduced by considering equation (10) and developing an expression for  $p$  therefrom (For details of such development, see Gopalakrishnan 1978). Under this treatment, the one-dimensional momentum equation can be written as

$$\frac{\partial U}{\partial t} + U \frac{\partial U}{\partial x} = -g \frac{\partial \eta}{\partial x} + f_v \quad (10)$$

where  $U$  is the mean horizontal velocity,  $\eta$  is the water level fluctuation from the still-water level (see Fig. 2) and  $f_v$  is the term to account for the vertical acceleration.

To include the effect of bottom friction in the run-up problem, drag force is introduced. Consider a water column with unit width and length  $l$  in the horizontal plane. The area of water in contact with the bottom is  $A = l \sec \alpha$  where  $\alpha$  is bottom slope. The drag force per element is therefore given by

$$F_D = C_D \rho (l \sec \alpha) V|V|/2 \quad (12)$$

where  $C_D$  is the drag coefficient and  $V = U \sec \alpha$  is the velocity along the bottom boundary. Since the total mass of water column is

$$M = \rho \int_0^{\ell} (\eta + h) dx \quad (13)$$

the friction force per unit mass,  $f_D$ , is  $f_D = F_D/M$ . It is noted that the velocity  $V$  is not the same throughout the element. As a first approximation, the mean velocity

$$V_m = \frac{1}{\ell} \int_0^{\ell} V dx \quad (14)$$

is used to evaluate  $f_D$ . Equation (11) is then modified to read

$$\frac{\partial U}{\partial t} + U \frac{\partial U}{\partial x} = - \frac{\partial \eta}{\partial x} + f_v - f_D \cos \alpha \quad (15)$$

where  $f_v$  is the term representing vertical acceleration when friction is included. In the above approach, the dimensionless drag coefficient  $C_D$  must be specified. In this study, a range of values of  $C_D$  is used to examine their effects on run-up. The final results shown in regard to the 1-D model are computed for  $C_D = 0.05$ .

In addition to momentum equations, the continuity equation

$$\frac{\partial u}{\partial x} + \frac{\partial w}{\partial z} = 0 \quad (16)$$

must be satisfied. Integrating equation (16) with respect to  $z$ , using the kinematic boundary condition  $D\eta/Dt = 0$ , the continuity equation reads

$$\frac{\partial \eta}{\partial t} + \frac{\partial}{\partial x} [U (h + \eta)] = 0$$

Equations (15) and (17) form the set of equations governing wave run-up.

### 3.2 Numerical Technique

Unlike the two-dimensional storm surge problem for offshore region where the application of the finite element method is straight-forward, wave run-up on land using finite element method involves a moving boundary at land-water interface and is difficult to handle. Since this problem constitutes a major part of this study, the manner in which run-up is handled is given below in some detail.

### 3.2.1 Finite element discretization

The equations governing wave run-up are equations (15) and (17). The dependent variables are  $\eta$  and  $U$  and the independent variables,  $x$  and  $t$ . Similar to the two-dimensional storm surge problem, the finite element procedure is adopted for space discretization only. This results in one-dimensional elements or line elements as shown in Fig. 3.

Examination of equations (15) and (17) shows that the first order spatial derivatives of  $\eta$  and  $U$  both have significant coefficients. It is therefore desirable to use higher order shape functions while applying the finite element technique. As is well known, under these circumstances, the Hermitian cubic shape function is eminently suited to the situation. Moreover, being a cubic polynomial, it can adapt itself to the "corrugations" on the water surface that occurs as water starts moving up the beach.

Applying the above numerical techniques, the governing equations reduce to two matrix equations as shown below:

$$[C_1] \{\dot{U}\} = \{B_1\} \quad (18)$$

$$[C_2] \{\dot{\eta}\} = \{B_2\} \quad (19)$$

Solution of these equations yields the time derivatives of  $U$  and  $\eta$ . The variables are then solved using the Euler Predictor-Corrector method for integration in time. Details of the description of the method are contained in Gopalakrishnan (1978).

### 3.2.2 Time dependent front element

The wave run-up problem has an upstream control section (the vertical plane  $x = 0$  shown in Fig. 3) and a downstream control section at the tip of the wedge of water on the sloping beach. The upstream control section remains unchanged in time. However, the downstream section has to move with the water-front. This is what characterizes wave run-up as a moving boundary problem in the one-dimensional system.

Let it be assumed that at time  $t$  the wave has reached the shoreline and is about to climb the beach as in Fig. 4. The last element (or the end-element) denoted as  $AB$  has a length  $l$  at time  $t$ . At time  $(t + \Delta t)$  the tip of water has moved up (Fig. 4). We let the last node move with the tip and take up the position  $B_1$  at  $(t + \Delta t)$ . The end-element length now is  $l_1$ , as shown in Fig. 5. In order to determine  $l_1$ , we consider the Lagrangian motion of water at the tip of the moving front. The distance " $s$ " which is equal to  $l_1 - l$  is given by:

$$s = U_e(t) \Delta t + \frac{1}{2} a (\Delta t)^2 \quad (20)$$

where  $U_e(t)$  is the velocity of the tip at time  $t$  and " $a$ " is its Lagrangian acceleration assumed constant in the interval  $\Delta t$ . The water level  $\eta$  at the tip of the front at time  $t + \Delta t$  is  $(s \cdot \tan \alpha)$  where  $\alpha$  is the angle of the beach slope to the horizontal plane. However, a more rigorous way of determining  $U$  and  $\eta$  at the tip in the present study is explained as we proceed further.

The approach adopted implies that the end-element has a length which is time-dependent. Moreover, its length keeps on increasing as the wave moves up the beach. If the end-element has a length much larger than the elements prior to it, then the global coefficient matrix tends towards becoming ill-conditioned. In order to avoid this, we split the end-element into two elements when its length exceeds the "regular" element length by a certain amount, say 20%. This means introducing a new node between the last two nodes. The values of the variable at the new node can be easily obtained by using the shape functions and the position of the new node between the last two nodes. This procedure is illustrated using Figs. 6-8.

After this step of splitting the end-element CD into the two elements CD and DE, the element CD remains constant in length and DE becomes the end-element with the node E now following the tip. By such a procedure we are able to have mobile elements at the end while avoiding the possibility of the coefficient matrix becoming ill-conditioned.

What dictates the flow on the downstream side is the ground slope and the velocity at the tip of the moving water. Let the velocity of water at the tip be  $U_e$  and the water level there  $\eta_e$ .

From Fig. 9 it is seen that the tip travels a horizontal distance  $s$  in the interval  $\Delta t$ . The mean velocity of the tip in the period between  $t$  and  $t + \Delta t$  is:

$$U_m = [U_e(t) + U_e(t + \Delta t)]/2 \quad (21)$$

Hence:

$$s = U_m \Delta t \quad (22)$$

From Fig. 9 it follows that:

$$\eta_e(t + \Delta t) = \eta_e(t) + s \tan \alpha \quad (23)$$

However, it is seen above that in the computation of  $\eta_e(t + \Delta t)$ ,  $U_e(t + \Delta t)$  is involved and that  $U_e(t + \Delta t)$  is unknown until all quantities for the instant  $(t + \Delta t)$  have been computed.

The value of the velocity  $U_e(t + \Delta t)$  can be predicted by considering the Lagrangian acceleration of the tip. Let the Lagrangian acceleration be "a" at the instant  $t$ .

Therefore:

$$U_e(t + \Delta t) = U_e(t) + a\Delta t \quad (24)$$

But 'a' itself is a function of  $t$ . Hence, during the predictor-corrector operation (adopted for moving ahead in time) the iterations take the mean of the total accelerations  $a(t)$  and  $a(t + \Delta t)$  into account.

The following steps explain the relationships during the iterations of the predictor-corrector:

$$a_e(t) = \frac{\partial}{\partial t} [U_e(t)] + U_e(t) \frac{\partial}{\partial x} [U_e(t)] \quad (25)$$

$$U_e(t + \Delta t) = U_e(t) + a_e \Delta t \quad (26)$$

$$U_m = [U_e(t) + U_e(t + \Delta t)]/2 \quad (27)$$

$$s = U_e(t) \Delta t + (1/2) a_e (\Delta t)^2 \quad (28)$$

$$\eta_e(t + \Delta t) = \eta_e(t) + s \tan \alpha \quad (29)$$

Using the above value of  $U_e(t + \Delta t)$  as the downstream boundary condition, all quantities for the instant  $t + \Delta t$  are computed. The iterations are continued till two successive values of  $U_e(t + \Delta t)$  differ by only a pre-set tolerance.

### 3.2.3 Wave Breaking

In general, storm waves break as they approach the shore. In mathematical modeling, wave-breaking is difficult to handle. A method is developed here which circumvents the breaking phenomenon but gives reasonably accurate values of wave surge height and intrusion distance. The method is based on the consideration that a flat coastal bottom causes waves to break while bottom slopes of about 0.3 or steeper have a tendency to reflect the waves or at least allow the waves to complete the run-up before breaking. Thus, if we scale the coordinates so that the bottom profile is transformed into one that is of moderately steep slope, then the numerical model may be run without encountering the breaking phenomenon. The results of such runs can then be transformed back to the original coordinates by applying the respective scales. In this study, the transformation is made assuming that wave steepnesses in the model and the prototype remain the same and so do the relative water depths.

In reference to Fig. 10, the horizontal scale is  $F_h = d_m/d_p$  and the vertical scale is  $F_v = h_m/h_p$  where  $d_p \approx 600$  m. Letting  $d_m = 10$  m and  $h_m = 3$  m, the horizontal scale is approximately 1/60 and the kinematic parameters, namely wave height  $H_m$ , wave length  $L_m$  and wave period  $T_m$  in the distorted model can be readily determined. That is, assuming  $h_m/L_m = h_p/L_p$  we have

$$L_m = L_p \frac{h_m}{h_p} \quad (30)$$

where  $L_p$  is the prototype wave length obtained from

$$L_p = \frac{gT_p^2}{2\pi} \tanh\left(\frac{2\pi h_p}{L_p}\right) \quad (31)$$

$T_p$  being the prototype wave period. Furthermore, since

$$L_m = \frac{gT_m^2}{2\pi} \tanh\left(\frac{2\pi h_m}{L_m}\right) \quad (32)$$

model wave period may be calculated. Finally, if it is assumed that wave steepnesses remain unchanged in the model and the prototype,

$$\frac{H_m}{L_m} = \frac{H_p}{L_p}$$

or

$$H_m = \frac{L_m}{L_p} H_p \quad (33)$$

#### 3.2.4 Boundary and initial conditions

The number of boundary conditions for a given problem depends on the number of equations in the mathematical system governing the physical situation and on the order of differential equations in that system. In the present model, the unknowns are two in number, namely,  $U$  and  $\eta$ , and the corresponding mathematical system consists of two equations, namely, equations (15) and (17). These equations are of the first order. Thus, we need two boundary conditions, one on  $\eta$  and one on  $U$  to solve the system. These two conditions are specified through:

- (1)  $\eta$  at the upstream boundary. That is, water elevation at  $x = 0$  must be specified for all time  $t$ .
- (2)  $U$  at the downstream boundary (while following the moving boundary) as indicated previously.

The initial conditions chosen for wave run-up are  $\eta = 0$  and  $U = 0$  at  $t = 0$  for all points in the domain.

#### 3.3 Movement of Storm Surge on Land

The movement of a water body over land due to storm surge is a much slower process compared to that due to waves. As a result, Coriolis force and wind stress become important factors to be considered. Hence, the following set of one-dimensional equations are used to analyze storm surge movement onto land:



$$\frac{\partial U}{\partial t} + U \frac{\partial U}{\partial x} - f_{\Omega} V_l = -g \frac{\partial \eta}{\partial x} - f_D + \frac{\tau_x^S / \rho}{(h+\eta)} \quad (34)$$

$$\frac{\partial \eta}{\partial t} + \frac{\partial}{\partial x} [U(h+\eta)] = 0 \quad (35)$$

where  $f_{\Omega} = 2\Omega \sin\phi$  is the Coriolis parameter (see equations (2) and (3)),  $f_D$  is the friction term (see equation (15)),  $\tau_x^S$  is the wind stress given by equation (6) and  $V_l$  is the longshore current.

The manner in which the above equations are discretized and the mobile finite element at the leading edge is treated remain essentially the same as that of wave run-up.

The mean low water plus the mean high tide (astro-tide) is used as datum. Initially,  $U$  and  $\eta$  are set equal to zero for all points. The value of  $\eta$  computed from the two-dimensional storm surge model, located at the upstream boundary is used as one of the boundary conditions. At the downstream boundary,  $U$  is specified as is done for wave run-up. It is mentioned that using the datum selected, the storm surge and wave run-up obtained is the one that would cause maximum flooding. Also, although it is realized that interactions exist between astronomical tide and storm surge, such is neglected in this study. It is felt that in view of the other approximations made, this procedure is acceptable.

In subsequent computations, we first use this one-dimensional moving boundary storm surge model to compute intrusion distance for some hypothetical situations and compare the result with that obtained using the two-dimensional model for storm surge considering the coast as rigid vertical walls and project the surge height onto the land horizontally. We found that the results agree with each other quite well. Thus, a decision is made that in computing flooding for the selected sections for the North Carolina coast, the two-dimensional model will be used instead of this one-dimensional moving boundary storm surge model.

#### 4. DATA COLLECTION

In order to provide input into the numerical models, data of hurricane characteristics, offshore and near-shore bottom profiles, tidal variation, storm wave characteristics and longshore currents are needed. Furthermore, for the purpose of validation, information regarding storm and wave surge and flooding extent must be made available. The Army Corps of Engineers, United States Geological Survey, National Oceanic and Atmospheric Administration and National Weather Service were contacted to obtain information of tidal fluctuations, hurricane parameters and waves. Some details regarding storm surge and extent of damage on North Carolina coast were obtained from the following publications:

1. 1979 issues of Shore and Beach.
2. 1955 report of the Council of Civil Defense of North Carolina on hurricane rehabilitation project (Griffin 1955).
3. "Basic Environmental Data Summary" of the U.S. Army Corps of Engineers Coastal Engineering Research Center, Field Research Facility, Duck, North Carolina, (Miller 1981).
4. "Coastal Flooding Storm Surge Model" by Tetra Tech., Inc., (Tetra Tech, Inc., 1981).

In addition, we consulted proceedings of the International Conference on Coastal Engineering (1976), proceedings of the American Society of Civil Engineers, Journal of the Waterways, Harbours, Coastal and Ocean Engineering Division, and the Journal of the American Meteorological Society, as indicated in the References.

#### 4.1 Hurricane Data

As mentioned earlier, we intend to use Hurricane Hazel of 1954 in our study as the forcing storm. Information regarding Hurricane Hazel was obtained from two sources: 1) "Climatological Data National Summary" of National Climate Center, National Oceanic and Atmospheric Administration (Seamon 1954), and 2) "Tropical Cyclones of the North Atlantic Ocean" of National Weather Service (Neumann 1978).

The hurricane center locations, according to Neumann (1978) are

date	time (E.S.T.)	latitude (N)	longitude (W)
Oct. 14	7:00 p.m.	28.7°	76.8°
Oct. 15	7:00 a.m.	32.8°	78.8°
Oct. 15	7:00 p.m.	41.3°	77.0°

Based on this information, the actual path is plotted in Fig. 11. For convenience of computation, the actual path is modified as shown by dotted lines in Fig. 11. The hurricane forward speeds  $V_f$  and direction  $\psi$  are computed accordingly for each of the two segments of the modified path and shown in the Figure. While there were no records of other hurricane parameters, according to a ship report in the vicinity of this area, it is estimated that  $A_p = 51.5$  mb and  $R_m = 20$  NM for the lower segment of the modified track and  $A_p = 65$  mb and  $R_m = 26$  NM for the upper segment.

#### 4.2 Offshore and Near-shore Profiles

The North Carolina coast is typified by two major coastal features: 1) a thin strip of Outer Banks backed by sounds, 2) the common land feature which rises steadily from the coastline. Six representative sections were chosen to examine storm surge and wave run-up and intrusion. The six sections are located near Brown Inlet, Kure Beach, Wilmington, Roanoke Island, Hampstead, and Cape Fear; their locations are shown in Fig. 20 identified by numbers enclosed in circles in the order given above. In Figs. 12 to 17, the exact locations of these sections are shown by arrows together with contour lines of bottom profile. Vertical profiles at these sections are obtained from USGS maps. To facilitate computation in the finite element models, these profiles are represented by

$$h = c_1 + c_2x + c_3x^2 + c_4x^3 \quad (36)$$

where  $h$  is water depth measured from still water level and  $x$  is considered positive towards the shore with origin at the offshore point (see Fig. 2). It is noted that data of these profiles are given for a distance which varies from approximately 1300 m to 2000 m depending on the location of the section (see Table 1). While subsequent computation of surge and wave run-up begins at 600 m from the shoreline, the determination of the coefficients of polynomial of these profiles utilizes entire data set. The coefficients  $c_1$ ,  $c_2$ ,  $c_3$ , and  $c_4$  are determined by the method of least squares and are given in Table 1. The resulting profiles are shown graphically in Figs. 18 (a, b, c, d, e, f). It should be mentioned that since data points of bottom profiles are rather sparse, the resulting profile given by the polynomials show humps at offshore points. This is especially noticeable at Cape Fear in Fig. 18f.

#### 4.3 Tidal Variation

The CERC Environmental Data Report (Miller 1981) gives details of time history of tidal range near Duck, North Carolina. A sample is shown in Fig. 19. For computation of propagation of storm surge in this study, an astronomical tide range value of 0.75 is added to mean low water.

#### 4.4 Wave Heights

There is no information of wave heights recorded near the coast during Hurricane Hazel. Wave heights during other storms, however, have been recorded at the CERC Field Research Facility at Duck, North Carolina, and reported (Miller 1981). During the December 1977 storm, the maximum wave height at the end of the Duck pier 600 m from shoreline is 4 m. Based on the same report, during storm Dennis, the maximum wave height is 3.4 m. For this study, it is assumed that wave height at section 1 (Fig. 2) is 4 m. Since no information of wave period for these storms is available, wave period is calculated using the formula suggested by the Shore Protection Manual (1973). That is, wave period is given by

$$T_s = 8.6 \exp\left(\frac{R_m \Delta p}{200}\right) \left(1 + \frac{0.104 \delta V_f}{U_R^{1/2}}\right)$$

where  $R_m$  (NM),  $\Delta p$  (inches of mercury) and  $V_f$  (knots) are as defined earlier;  $\delta$  is a coefficient depending on the forward speed  $V_f$  of the hurricane - taken as 1.0 for a slowly moving hurricane;  $U_R$  is the maximum sustained wind speed in knots and is given by  $U_R = 0.865 U_{\max} + 0.5 V_f$ , where  $U_{\max}$  is wind speed at  $R = R_m$ , given by  $U_{\max} = 0.868 [73 (\Delta p)^{1/2} - R_m (0.575 f_\Omega)]$  with  $f_\Omega$  being the Coriolis parameter. In this study,  $R_m = 26$  NM,  $\Delta p = 65$  mb (1.92 inches of mercury),  $V_f = 43$  knots and  $\delta = 1.0$ . Thus,  $T_s$  is computed to be 15.4 seconds approximately.

#### 4.5 Longshore Current

Again, there is no information in this regard for Hurricane Hazel. Birkemeier (1979) gives a maximum of 0.8 m/sec current velocity as observed during the December 1977 storm. In the present study, longshore current velocity of 1.0 m/sec is used in the one-dimensional model for surge.

#### 4.6 Storm Surge

Details of the storm surge due to four hurricanes - Hazel, Connie, Diane and Ione, from 1954 to 1955, are given in the publication of the Council of Civil Defense (Griffin 1955). Information from the publication is reproduced in Fig. 20. In Fig. 20, the run-up due to those hurricanes clearly is indicated. Of the six sections under consideration in this study, run-up values can be delineated for four locations. These values are given in Table 2 for comparison with computed results. Also, according to the report, Hurricane Hazel produced the highest storm surge-wave elevation of 14.7 ft. (4.4 m) above mean sea level at Holden Beach. Birkemeier (1979) reported values of storm surge near the CERC Pier at Duck, North Carolina, for the December 1977 storm; these values are comparable to those due to Hazel.

#### 4.7 Flooding Extent

This is one of the areas where systematic data collection is lacking. The Council of Civil Defense report (Griffin 1955) gives approximate extent of flooding at various regions along the North Carolina coast. Based on the information provided by the report, approximate flood areas (in shaded areas) are given in Figs. 11 to 16.

### 5. COMPUTATIONS

#### 5.1 Storm Surge Offshore

The six sections on the coast of North Carolina under study are shown in Fig. 18 marked 1 to 6. The computation of flooding is by means of the two-dimensional storm surge model for the offshore region and one-dimensional models for storm surge and storm wave run-up in the near-shore region (see comments at end of section 3 regarding storm surge computation). To save computational time, an offshore region is marked off the coast in the vicinity of Cape Hatteras as shown in Fig. 21 to compute the surge due to Hurricane Hazel. While developing the finite element grid, it is necessary to extend the grid beyond the shelf in order not to miss the shelf effects. In the present case, a distance of about 100 km offshore is considered. In addition to the modified track of Hurricane Hazel shown in Fig. 11, we introduce three hypothetical paths denoted by HZ1, HZ2, and HZ3 as shown in Fig. 11. Below latitude  $33^{\circ}$  N, the hurricane parameters are  $\Delta p = 51.5$  mb,  $R_m = 20$  NM and  $V_f = 13.3$  m/s. Above that latitude,  $\Delta p = 65$  mb,  $R_m = 26$  NM and  $V_f = 22.1$  m/s. In both cases,  $\psi = 90^{\circ}$ . Typical grid layouts for the finite element model are shown in Fig. 22. Several grid sizes were used to ensure accuracy. Typical time histories of storm surge due to HZ0 at Ocracoke, Hatteras, and Nags Head are shown in Figs. 25 (a), (b), and (c). Also, the time histories of storm surge for HZ1, HZ2, and HZ3 at these locations are shown in Fig. 26 to Fig. 28. It is found that HZ1 produces the maximum surge height of 1.8 m.

We also used a region south of Hatteras shown in Fig. 23; its finite element grid layout is shown in Fig. 24. Since HZO is closer to Cape Fear, which is our point of interest, we used only HZO as input for this region. The maximum surge height is found to be 1.5 m. In subsequent study of storm surge and wave run-up for the six sections selected, the storm surge height of 1.5 m is applied uniformly.

In applying the two-dimensional finite element model for storm surge computation, time step was varied from 100 seconds to 200 seconds and the CPU time used for analyzing the 18 hours of real time storm was approximately five minutes on the IBM 370/165 computer.

## 5.2 Storm Surge and Wave Run-up

Using a storm surge height of 1.5 m, astronomical tide of 0.75 m, wave height of 4 m and wave period of 15.4 seconds, the one-dimensional models for storm surge and wave propagation near-shore and on land are applied to the six selected sections using the bottom profile given in Table 1.

The storm surge intrusion, wave intrusion, total intrusion and maximum run-up as computed for the sections are given in Table 2. Included in Table 2 is also the maximum land elevation extracted from USGS contour maps.

In these computations, time step was 0.05 seconds and the CPU time is approximately 1 minute for each run.

## 6. VALIDATION

The results of our computation are compared with experimental values where applicable and with field observations where available. The offshore model had already been verified for Massachusetts Bay as reported by Wang and Connor (1975) and for the Virginia coast by Chen (1978). The validation of near-shore models are carried out using laboratory experimental results and field observations.

Apart from comparison with the above data, the soundness of these models is tested by changing grid sizes and time steps.

### 6.1 Comparison with Experiment

Horikawa (1978) gives experimental values for wave run-up from several sources. The data summarized in the form of a plot on page 111 (plot 2.10.2 a) of this reference is reproduced as shown in Fig. 29. In this figure,  $R$  is the wave run-up,  $H_0$  is the deep water wave height,  $L_0$  is the deep water wave length,  $h$  is the water depth at the toe of the sloping beach, and  $\alpha$  is the slope of the beach.

In the present verification, it is assumed that a progressive wave approaches the beach toe of water depth  $h = 9.84$  ft. with wave height  $H = 3.28$  ft. and the wave period  $T = 6.0$  sec. In order to compare the model wave run-ups with the experimental results of Fig. 29, the corresponding wave characteristics at deep water condition must be found. The steps are described as follows.

By the small amplitude wave theory, the relationship between the wave length, wave period, and water depth for shallow water condition can be stated as

$$L = \frac{gT^2}{2\pi} \tanh \frac{2\pi h}{L}$$

where  $L$  is the shallow water wave length,  $T$  is the period,  $h$  is the water depth and  $g$  is the gravitational acceleration. Entering the wave parameters mentioned above, the corresponding wave length is found to be  $L = 100$  ft. Thus, we have the relative water depth,  $h/L = 0.098$ , and the wave steepness,  $H/L = 0.033$ .

The wave length and the wave height at deep water can be found, from the appendix table of Shore Protection Manual (CERC 1973), if the shallow water relative water depth ( $h/L$ ) is known. For  $h/L = 0.098$ , the corresponding  $h/L_0$  is 0.054 and  $H/H_0$  is 1.011. Thus,

$$\frac{H_0}{L_0} = \frac{H/1.011}{h/0.054} = \frac{3.28/1.011}{9.84/0.054} = 0.018$$

Therefore, the plot indicated above is the relevant one. The comparison of wave run-ups between the numerical model and experimental results, for two beach slopes  $\cot \alpha = 3.33$  and  $\cot \alpha = 4.00$ , are shown below.

Cot $\alpha$	Run-up from Num. Model	R/H	R/H from Plot
3.33	7.03 ft.	2.14	2.1
4.00	6.57 ft.	2.00	1.85

The comparison brings out the efficiency of the numerical model. The run-up values above are taken from the output for the instant just before the onset of breaking as indicated by the numerical instability.

## 6.2 Comparison with Field Observations

Based on the publication of the Council of Civil Defense (Griffin 1955), observed run-up values at Kure Beach, Wilmington, Hampstead, and Cape Fear during Hazel are entered in Table 2. In reference to Fig. 20, it is seen that for Section 6, near Cape Fear, the model run-up result (3.09 m) agrees with the observed data (3.5 m). The values of maximum surge are over-estimated in Sections 2, 3 and 5. This is because the one-dimensional models used the same storm surge computed at Cape Fear, namely, 1.5 m as input. Since these sections are further removed from the Hurricane Hazel path than Cape Fear is, the storm surge at these locations is more likely to be less than that of Cape Fear. There are no field data in Sections 1 and 4 to compare with. However, the Council of Civil Defense (Griffin 1955) reported that most lands of North Carolina coast that were less than ten feet above sea level were covered by salt water. Our results of 4.25 m and 3.26 m are in agreement with his observations at these two sections. It is also seen

that the maximum run-up exceeds the maximum land elevation in Sections 4, 5 and 6. That is, overtopping results in those areas. Especially, it is noted that all the Outer Banks barrier islands will be totally flooded in the case of hurricane with the same magnitude as Hazel passing through.

It is concluded that the models developed in this study are useful and reliable tools for the determination of flooding extent due to storms on coastland. The safe set-back line for particular coastal areas can be determined by the models when the wave climate and hurricane characteristics are provided.

## REFERENCES

- Birkemeir, W. A., 1979. "The Effects of the 19 December 1977 Coastal Storm on Beaches in North Carolina and New Jersey," Shore & Beach, January, 1979.
- Chen, H. S., 1978. "A Finite Element Storm Surge Analysis and its Application to a Bay-Ocean System: Chesapeake Bay," Report No. 189, Applied Science and Ocean Engineering, Virginia Institute of Marine Science, Gloucester Point, Virginia.
- Damsgarrd, A. and Dinsmore, A. F., 1975. "Numerical Simulation of Storm Surges in Bays," Modeling 75, Symposium of Modeling Techniques, Proceedings of the American Society of Civil Engineers.
- Finlayson, B. A., 1972. The Method of Weighted Residuals and Variational Principles, Academic Press, New York, N.Y.
- Gallagher, R. H., Oden, J. T., Taylor, C. and Zienkiewicz, D. C., 1975. Finite Element in Fluids, Vol. 1 and 2, John Wiley & Sons, New York, N.Y.
- Gopalakrishnan, T. C., 1978. "Galerkin Finite Element Analysis of Wave Shoaling and Run-up," Ph.D. Thesis, North Carolina State University, Raleigh, North Carolina.
- Griffin, F. E., 1955. "Long-Range Hurricane Rehabilitation Project," Report, The Council of Civil Defense, Department of Administration of North Carolina, Raleigh, North Carolina.
- Horikawa, K., 1978. Coastal Engineering, John Wiley & Sons, New York, N.Y.
- Jelesnianski, C. P., 1967. "Numerical Computations of Storm Surges with Bottom Stress," Monthly Weather Review, Vol. 95, No. 11.
- Jelesnianski, C. P., 1974. "SPLASH - Special Program to List Amplitude of Storm Surge from Hurricane, Part II - General track and Variant Storm Conditions," Technical Memorandum, NWS TOL 52, National Weather Service, National Oceanic and Atmospheric Administration, U.S. Department of Commerce, Washington, D.C.
- Jelesnianski, C. P., 1976. "A Sheared Coordinate System for Storm Surge Equations of Motion with a Mildly Curved Coast," Technical Memorandum, NWS TDL 61, National Weather Service, National Oceanic and Atmospheric Administration, U.S. Department of Commerce, Washington, D.C.
- Miller, H. C., 1981. Basic Environmental Data Summary, Field Research Facility, Coastal Engineering Research Center, Army Corps of Engineers, Duck, North Carolina.
- Neumann, C. J., Cry, G. W., Caso, E. L., and Jarvinen, B. R., 1978. "Tropical Cyclones of the North Atlantic Ocean," National Weather Service, National Oceanic and Atmospheric Administration, U.S. Department of Commerce, Washington, D.C.



- Pagenkopf, J. R. and Pearce, B. R., 1976. "A User's Manual for CAFE-1; A Two-Dimensional Finite Element Circulation Model," Ralph M. Parson Laboratory, Report No. 217, Massachusetts Institute of Technology, Cambridge, Massachusetts.
- Pearce, B. R., 1972. "Numerical Calculation of the Response of Coastal Waters to Storm System," Technical Report No. 12, Coastal and Oceanographic Engineering Laboratory, University of Florida, Gainesville, Florida.
- Reid, R. O. and Bodine, B. R., 1968. "Numerical Model for Storm Surges in Galveston Bay," Journal of the Waterway and Harbours Division, Proceedings of the American Society of Civil Engineers, WW1, February.
- Seamon, L. H., 1954. "Climatological Data National Summary," National Climate Center, National Oceanic and Atmospheric Administration, U.S. Department of Commerce, Washington, D.C.
- Shore Protection Manual, 1973. Publication of the Coastal Engineering Research Center, U.S. Army Corps of Engineering, Washington, D.C.
- Taylor, C. and Davis, J., 1975. "Tidal and Long Wave Propagation - a Finite Element Approach," Computers and Fluids, Vol. 3.
- Tetra Tech, Inc., 1981. Coastal Flooding Storm Surge Model, Report to Federal Insurance Administration, Pasadena, California.
- Wang, J. D. and Connor, J. J., 1975. "Mathematical Modeling of Near Coastal Circulation," Ralph M. Parsons Laboratory, Report No. 200, Massachusetts Institute of Technology, Cambridge, Massachusetts.
- Wanstrath, J. J., 1977. "Nearshore Numerical Storm Surges and Tidal Simulation," Report No. H-77-17, U.S. Army, Waterways Experimental Station, Vicksburg, Mississippi.
- Yeh, G. T. and Chou, F. K., 1979. "Moving Boundary Numerical Surge Model," Journal of the Waterway, Port, Coastal and Ocean Division, Proceedings of the American Society for Civil Engineers, WW3, August.

Table 1. Coefficients of polynomials representing bottom profiles of six sections

Station	Profile Coefficients*				Distance (m) to shoreline from section 1 (Fig. 2)
	C <sub>1</sub>	C <sub>2</sub>	C <sub>3</sub> (x10 <sup>-5</sup> )	C <sub>4</sub> (x10 <sup>-8</sup> )	
1 Brown Inlet	9.5750	-0.0109	2.2629	-1.3092	1512
2 Kure Beach	10.6516	0.0022	-0.1626	-0.0913	2088
3 Wilmington	11.0853	-0.0070	1.0626	-0.5101	1944
4 Roanoke Is.	11.3717	-0.0095	-0.5886	-0.4074	1320
5 Hampstead	12.0057	-0.0103	1.3843	-0.6039	1968
6 Cape Fear	6.8011	-0.0145	1.8729	-0.6561	2040

\* Depth is given by the equation  $h = C_1 + C_2X + C_3X^2 + C_4X^3$  where X is measured from the offshore point ( $X \neq 0$ )<sup>2</sup> towards the shore.

Table 2. Intrusion distance for the six sections

Station	Storm Surge Intrusion (m)	Wave Intrusion (m)	Total Intrusion (m)	Maximum Run-up (m)	Observed Run-up (m)	Maximum Land Elevation (m)
Brown Inlet	53.9	71.2	125.1	4.25		7.7
Kure Beach	124.2	112.1	236.3	3.65	2.7	4.6
Wilmington	93.8	90.6	184.4	4.12	2.7	4.6
Roanoke Is.	117.2	93.6	210.8	3.26		2.2
Hampstead	54.7	87.6	114.3	4.14	3.1	3.1
Cape Fear	80.5	64.2	144.7	3.09	3.5	3.1

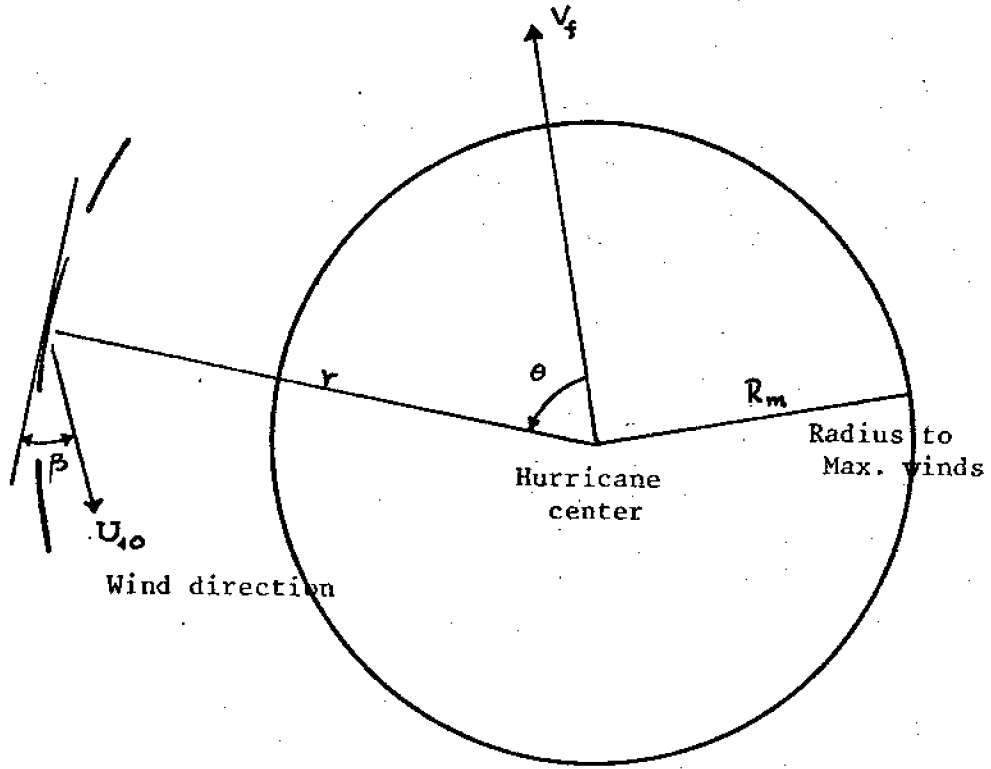


Figure 1. Hurricane parameters

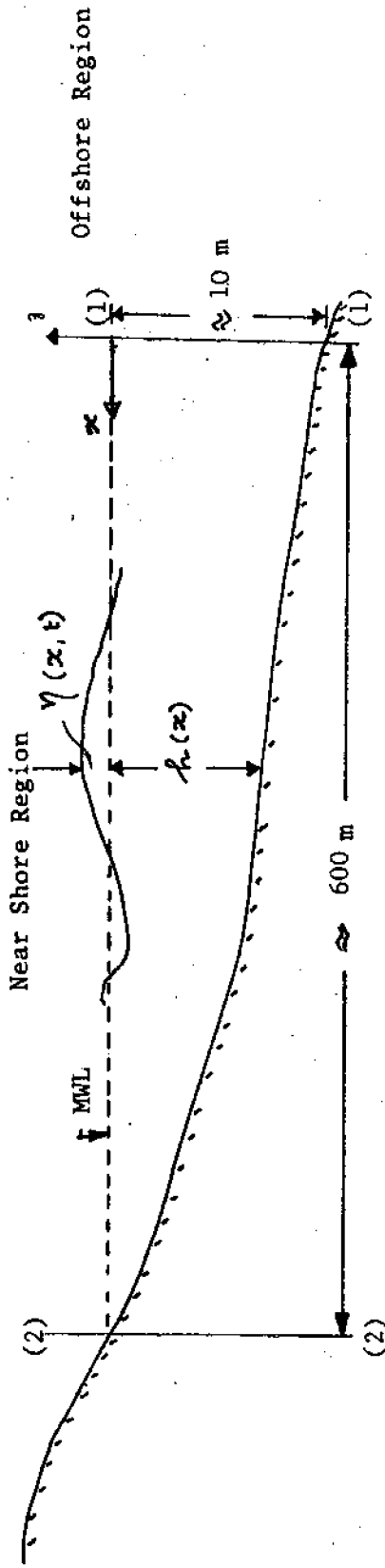


Figure 2. Near shore region

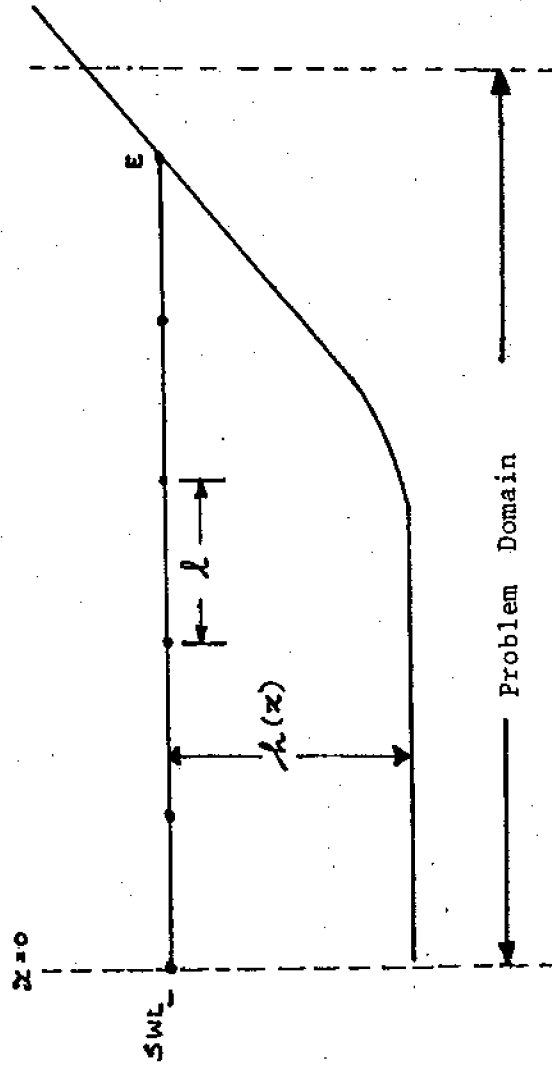


Figure 3. Spatial discretization

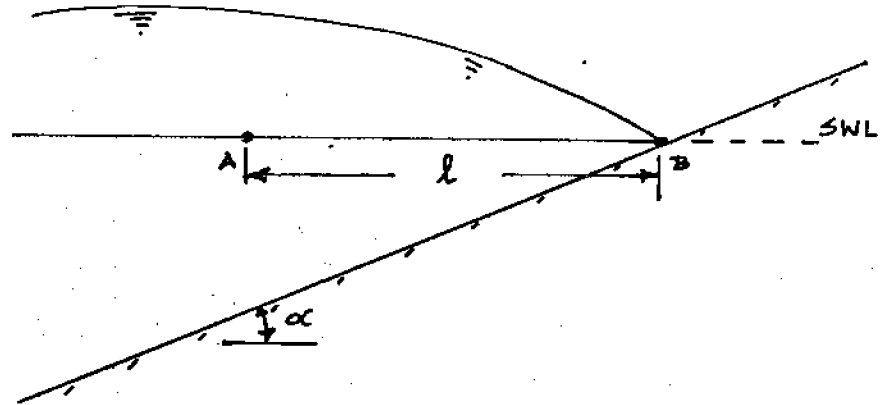


Figure 4. Water profile and end-element at time  $t$

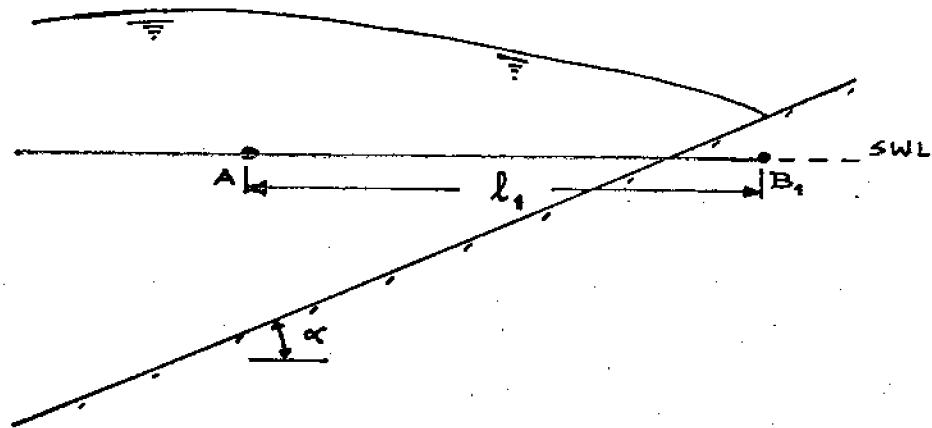


Figure 5. Water profile and end-element at time  $t + \Delta t$

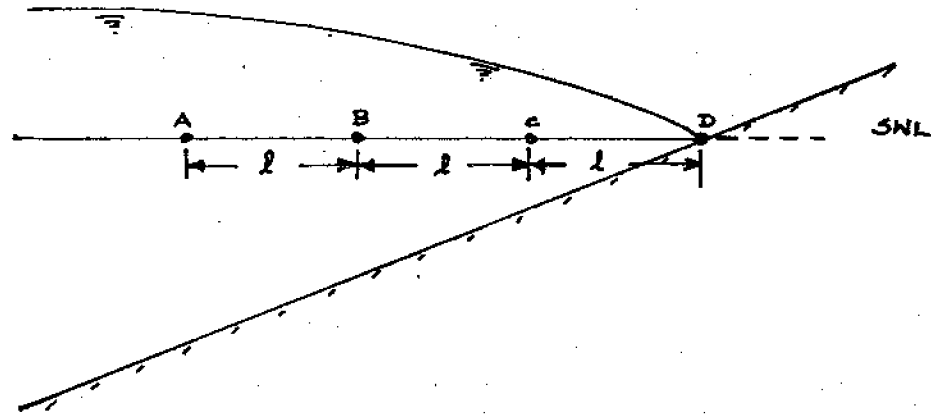


Figure 6. Position at time  $t$

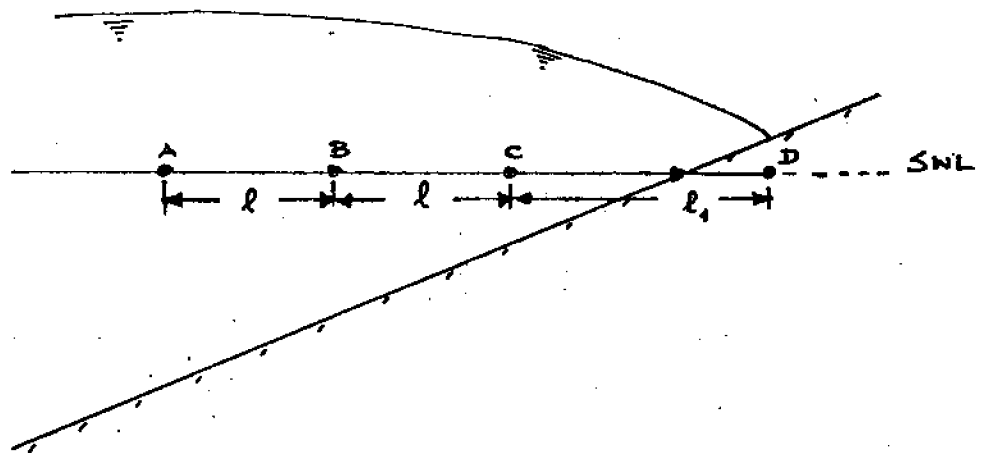


Figure 7. Position at time  $t + \Delta t$



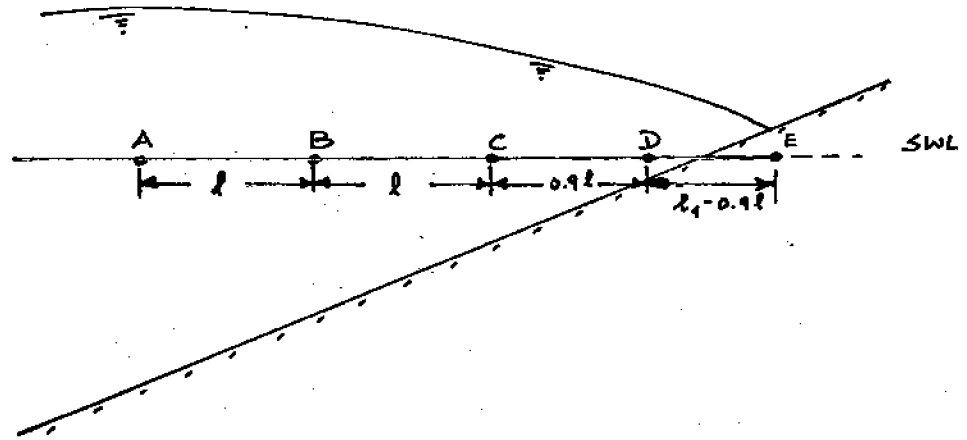


Figure 8. Element splitting at time  $t + \Delta t$

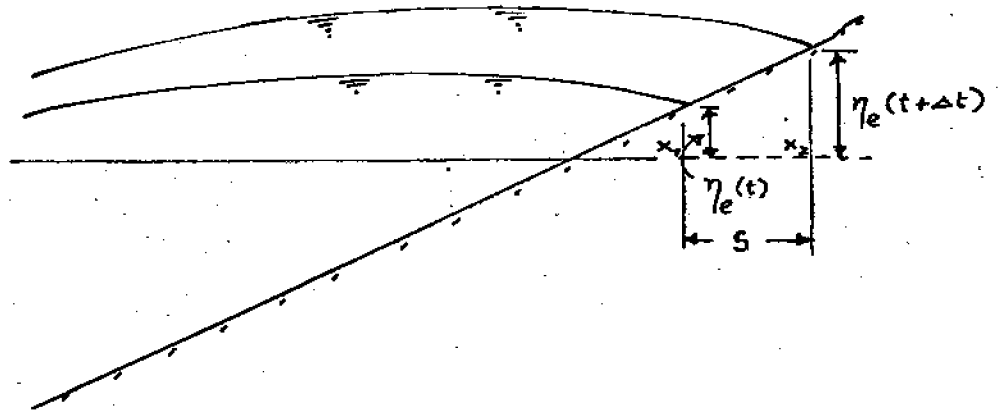


Figure 9. Downstream conditions at the instants  $t$  and  $t + \Delta t$

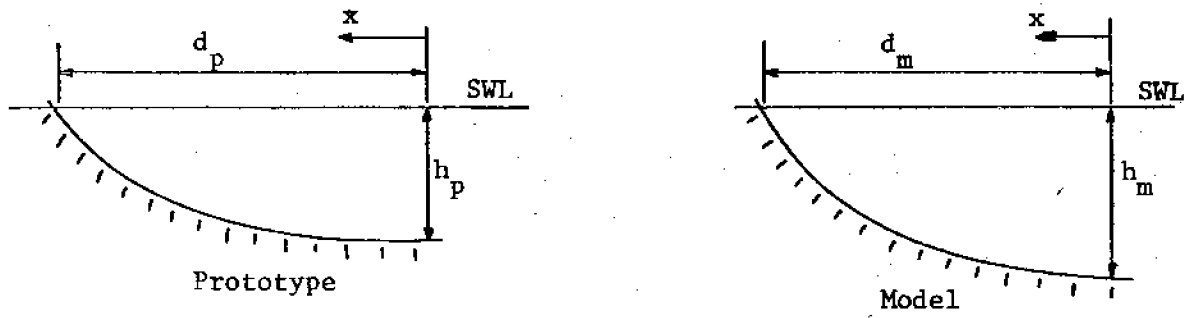


Figure 10. Definition sketch (distorted scale model)

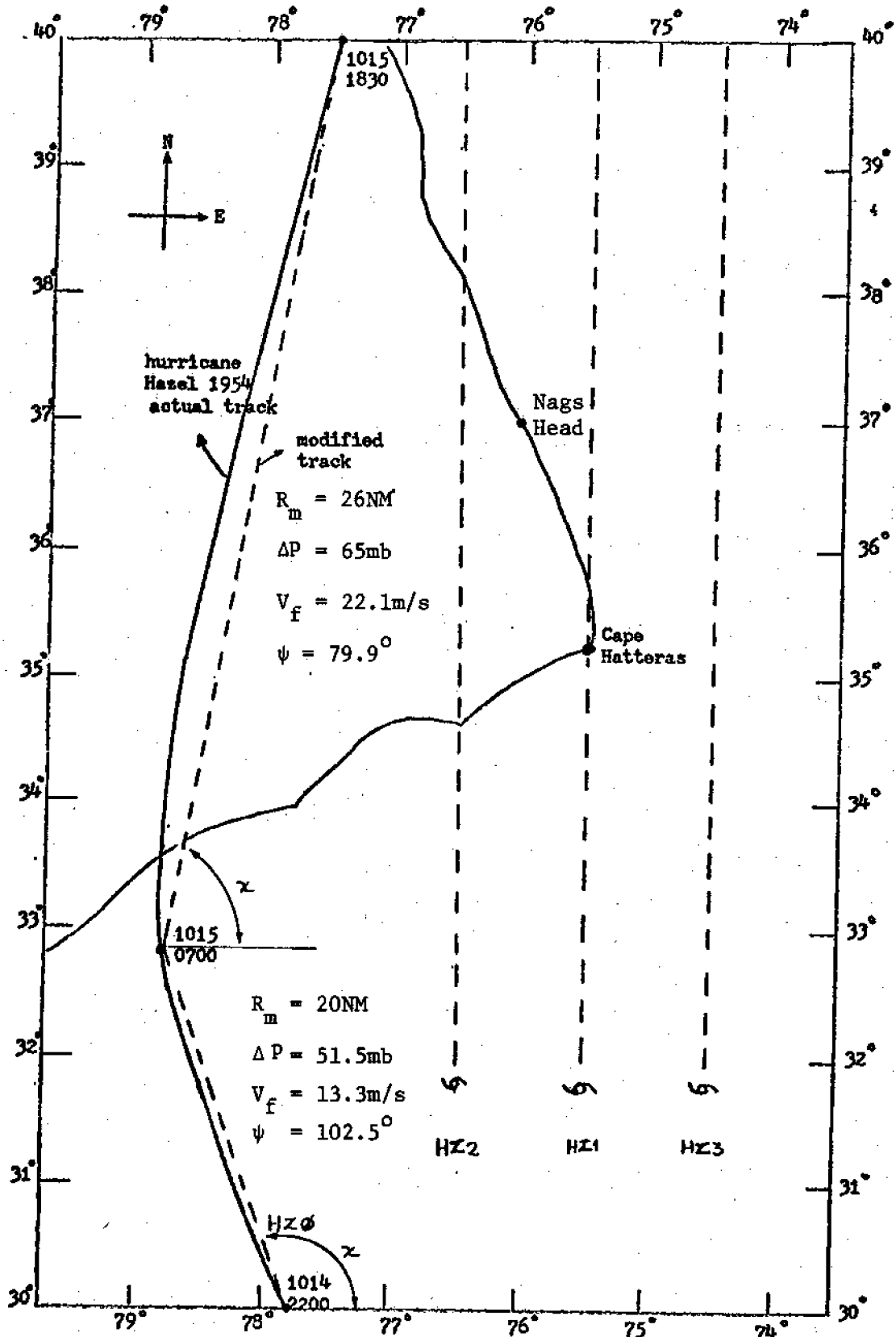


Figure 11. Actual and hypothetical paths of Hurricane Hazel

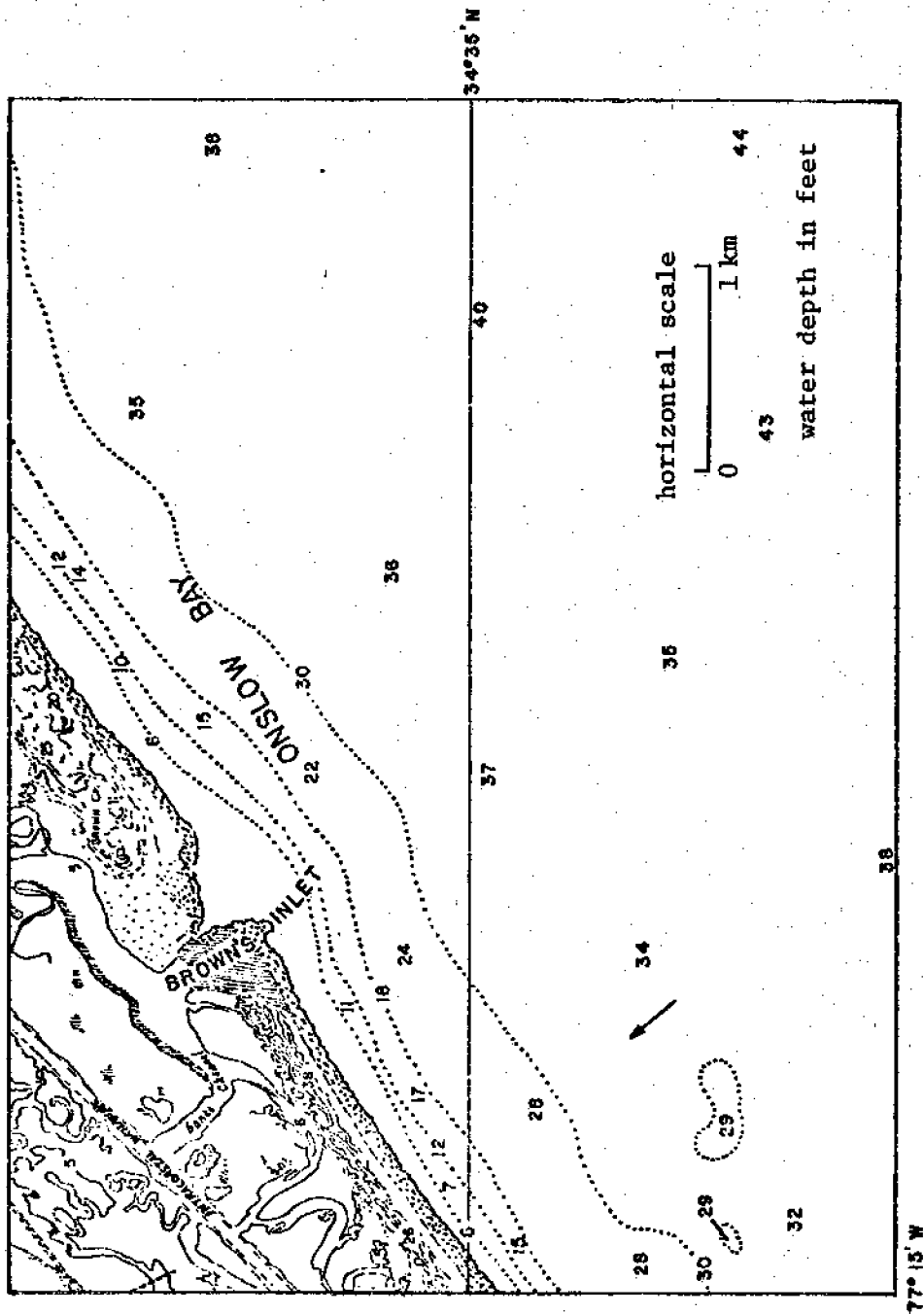


Figure 12. Region 1 : Brown Inlet

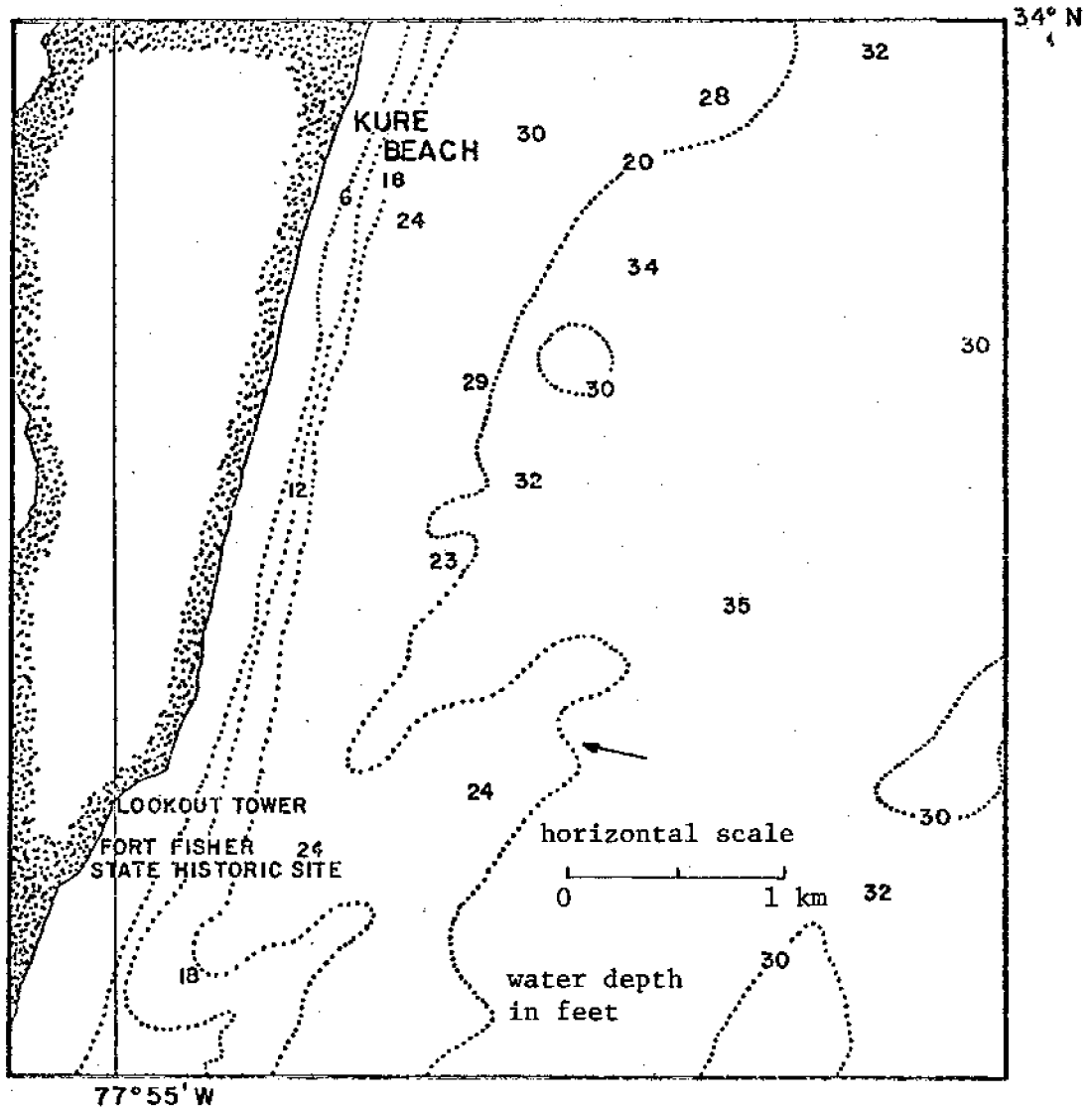


Figure 13. Region 2 : Kure Beach

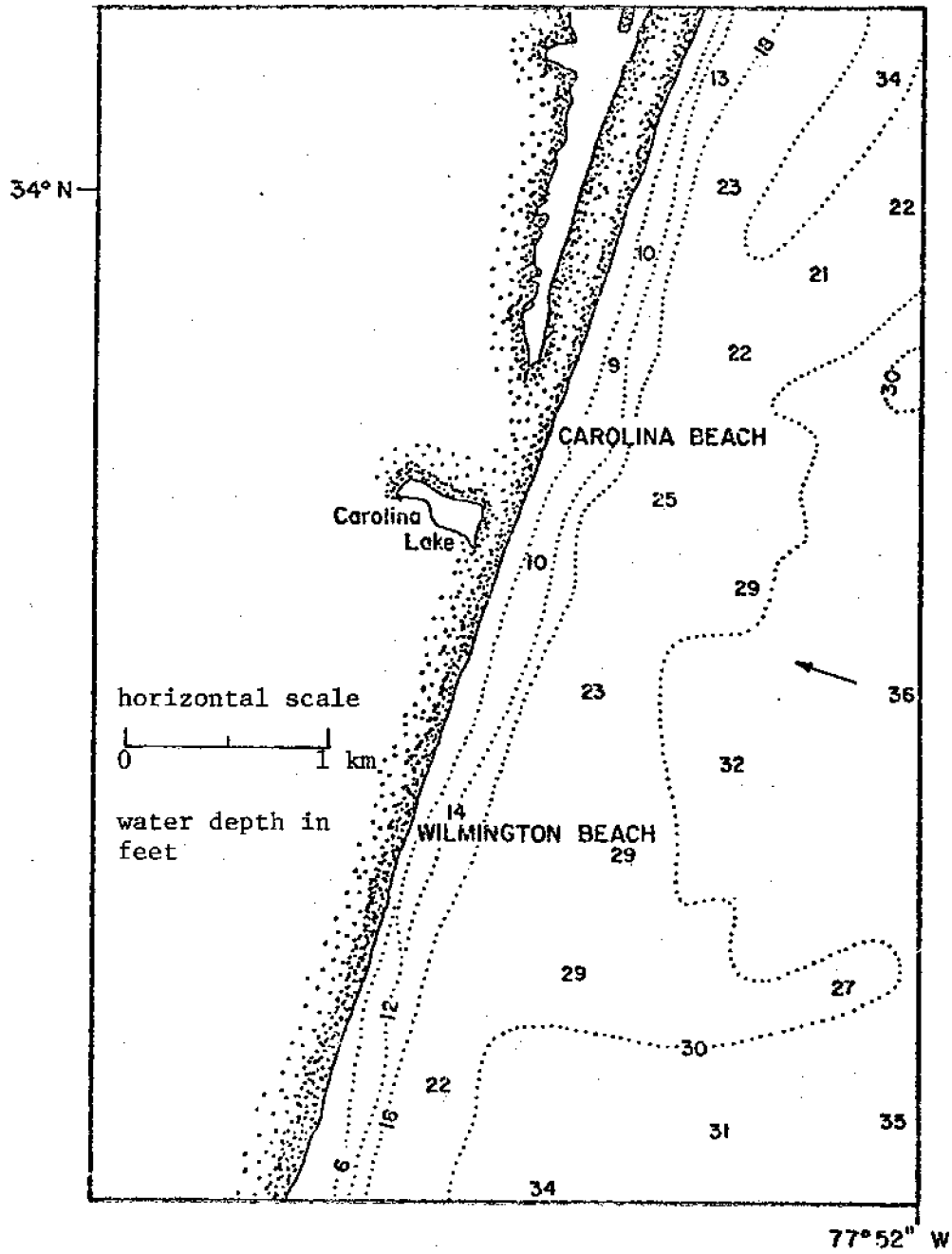


Figure 14. Region 3 : Wilmington Beach

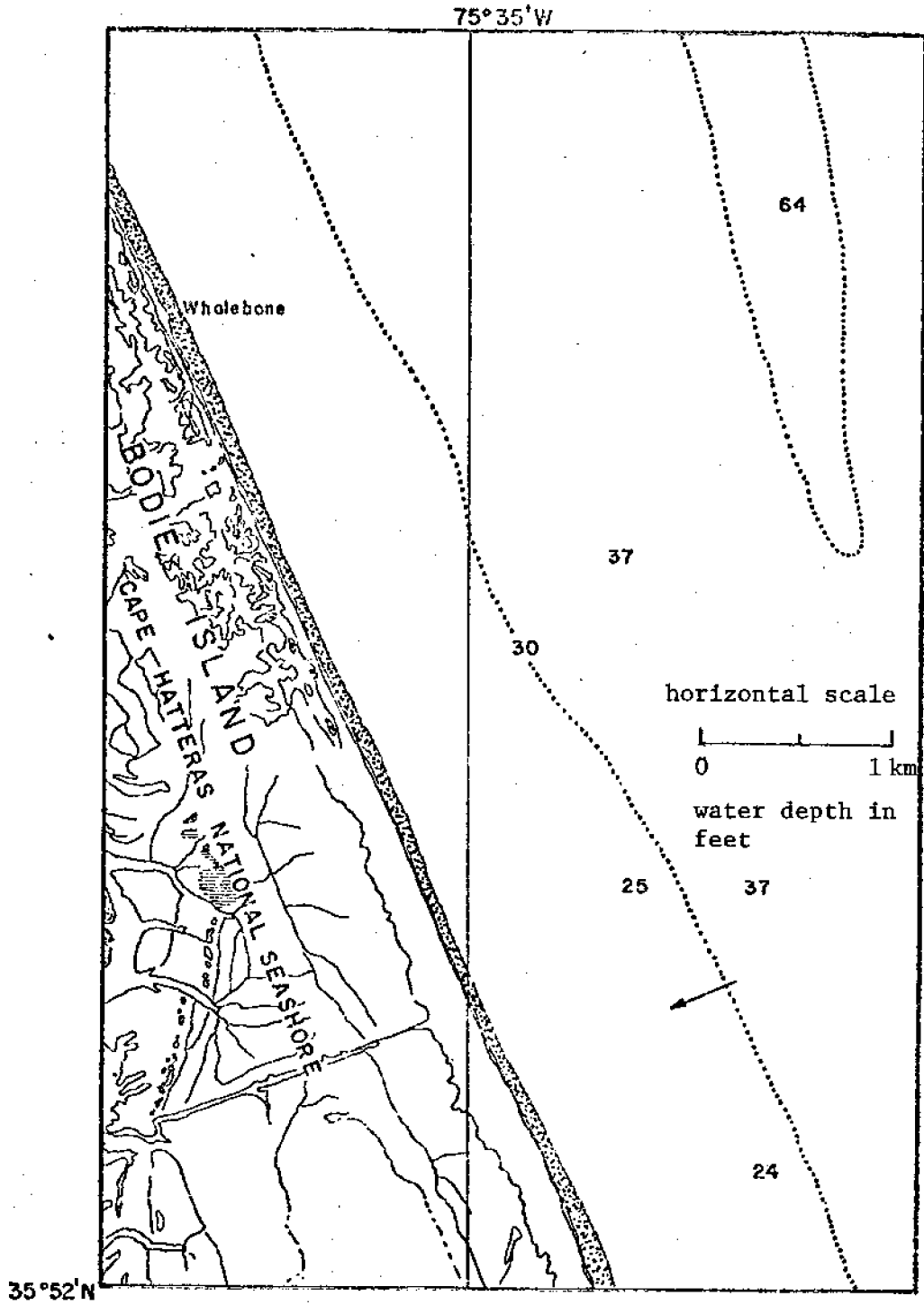


Figure 15. Region 4 : Roanoke Island

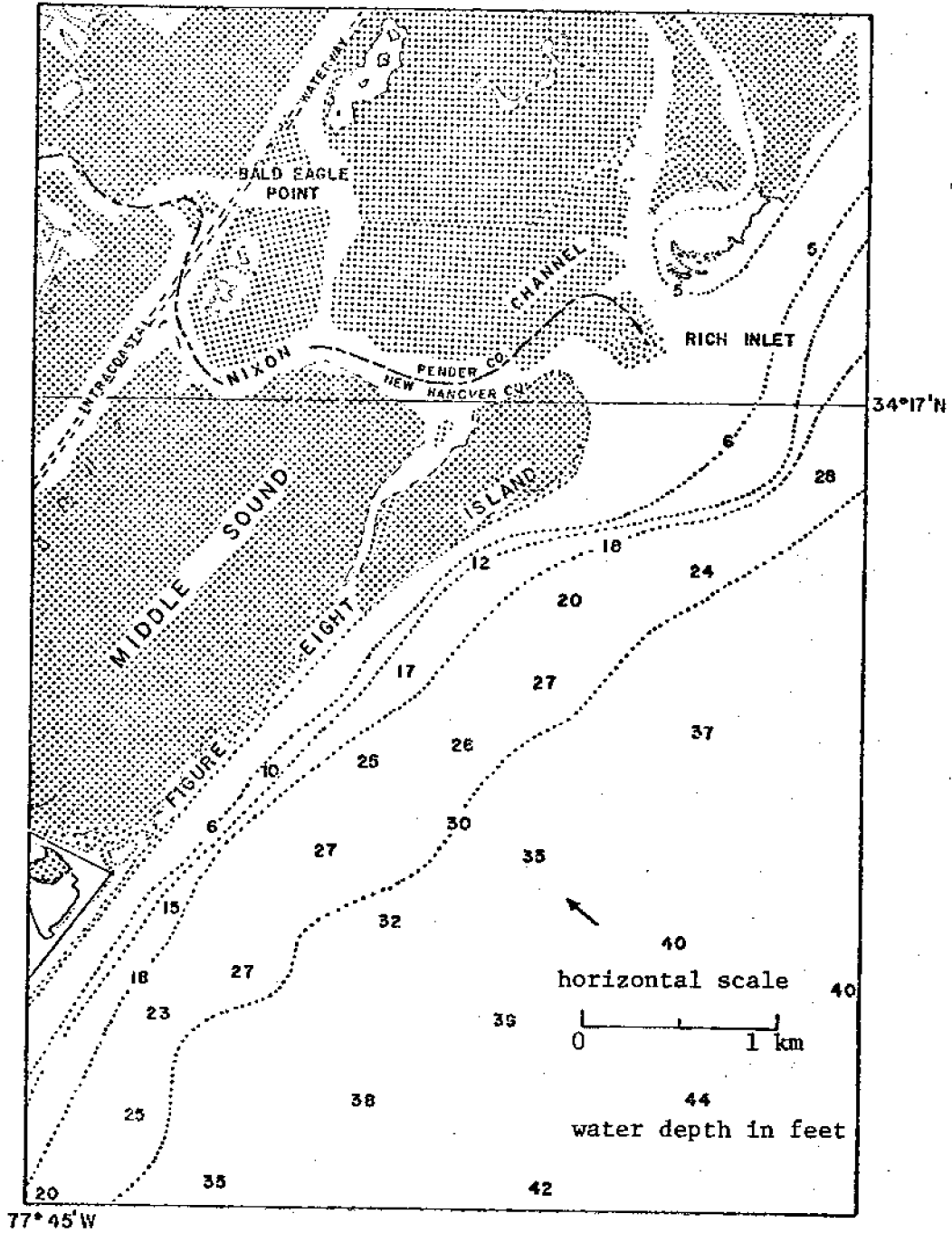


Figure 16 . Region 5 : Hampstead



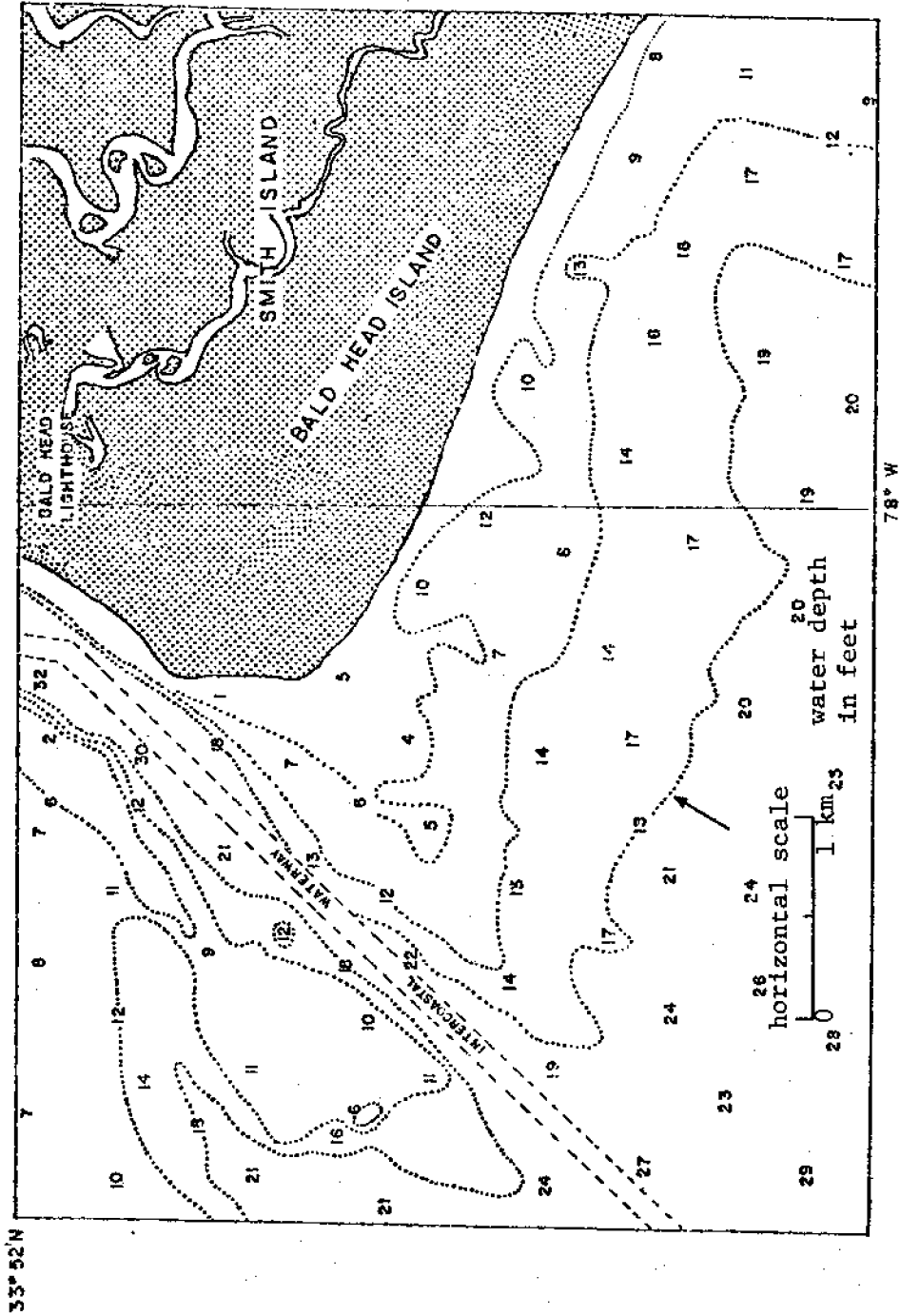


Figure 17. Region 6 : Cape Fear

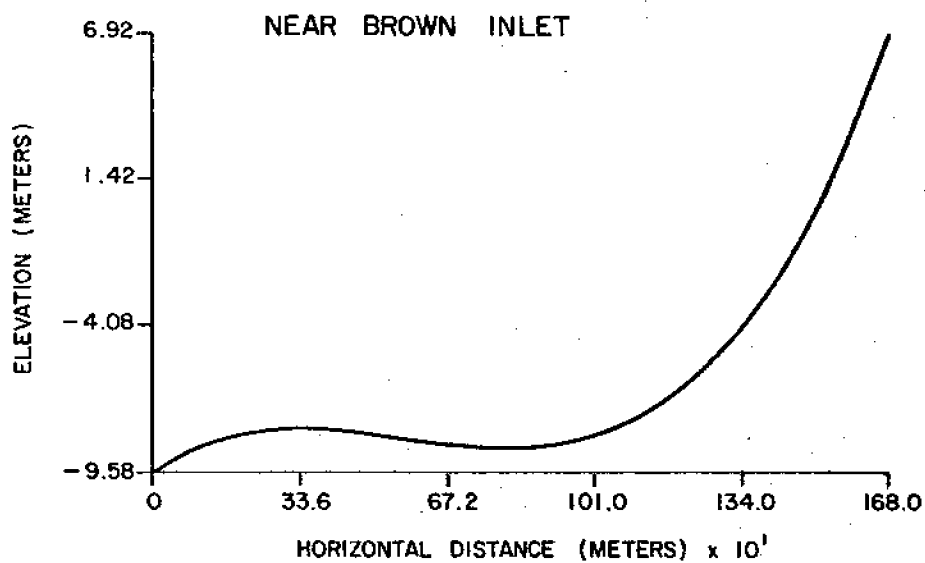


Figure 18 (a). Bottom profile near Brown Inlet

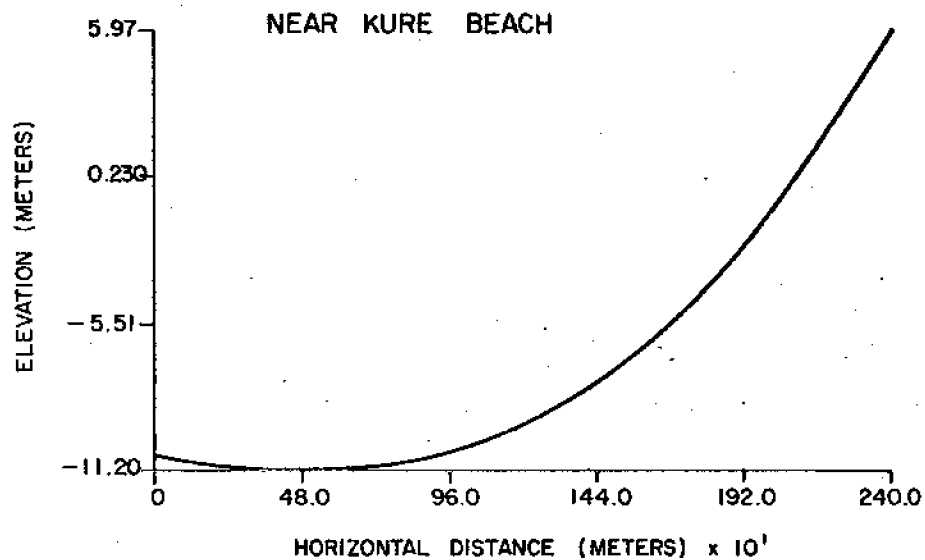


Figure 18 (b). Bottom profile near Kure Beach

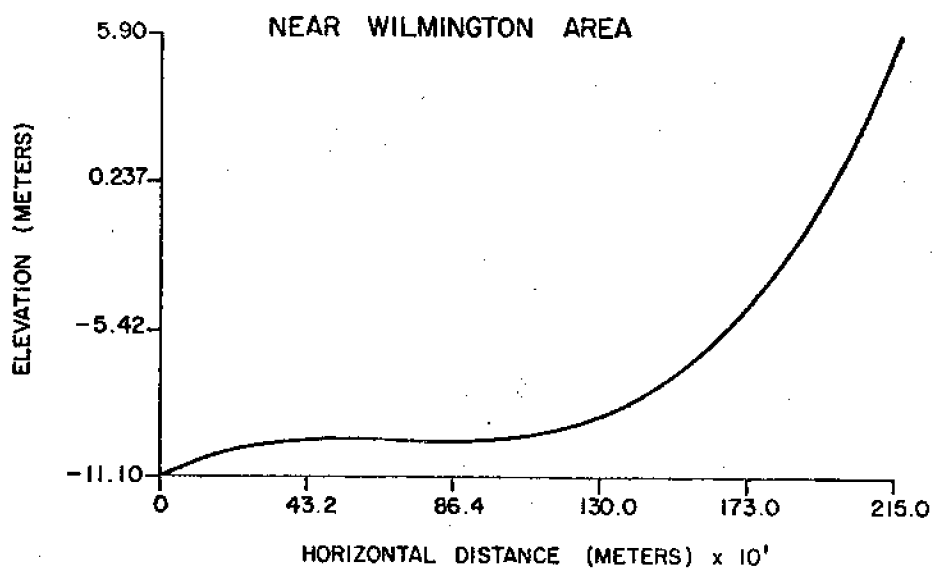


Figure 18 (c). Bottom Profile near Wilmington

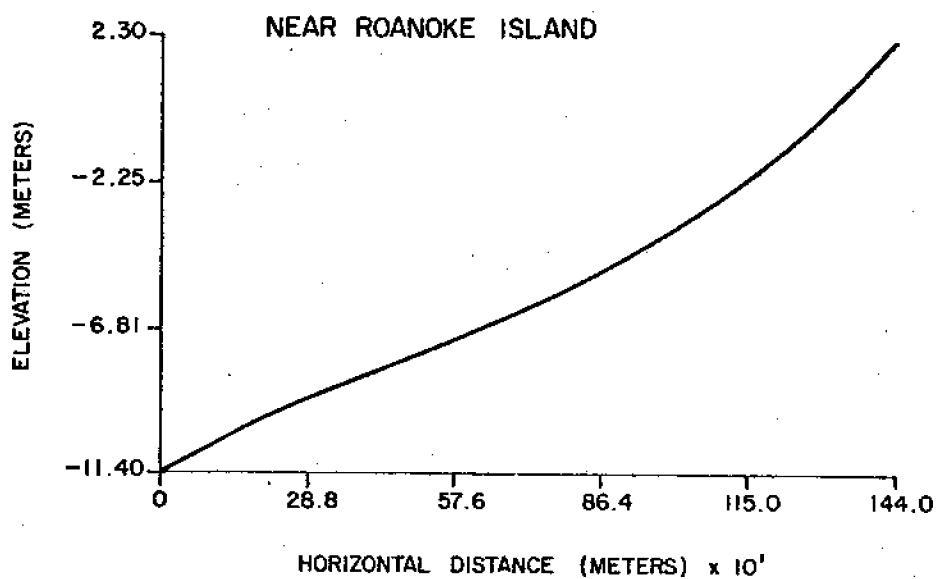


Figure 18 (d). Bottom profile near Roanoke Island

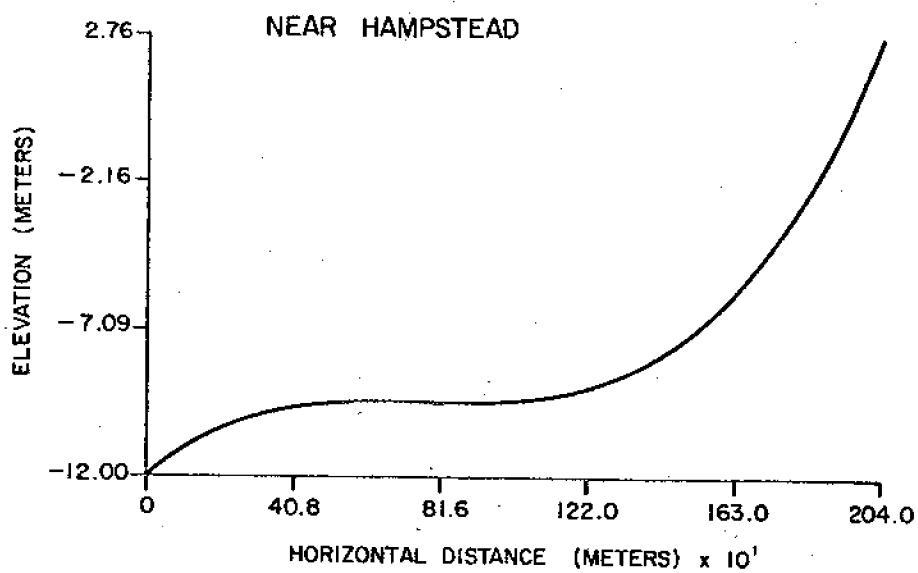


Figure 18 (e) Bottom profile near Hampstead

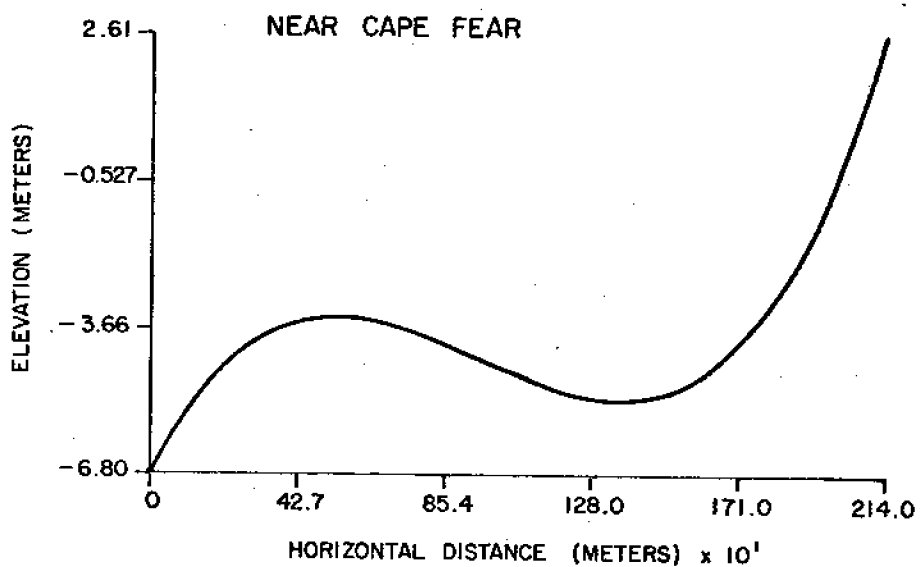


Figure 18 (f). Bottom profile near Cape Fear

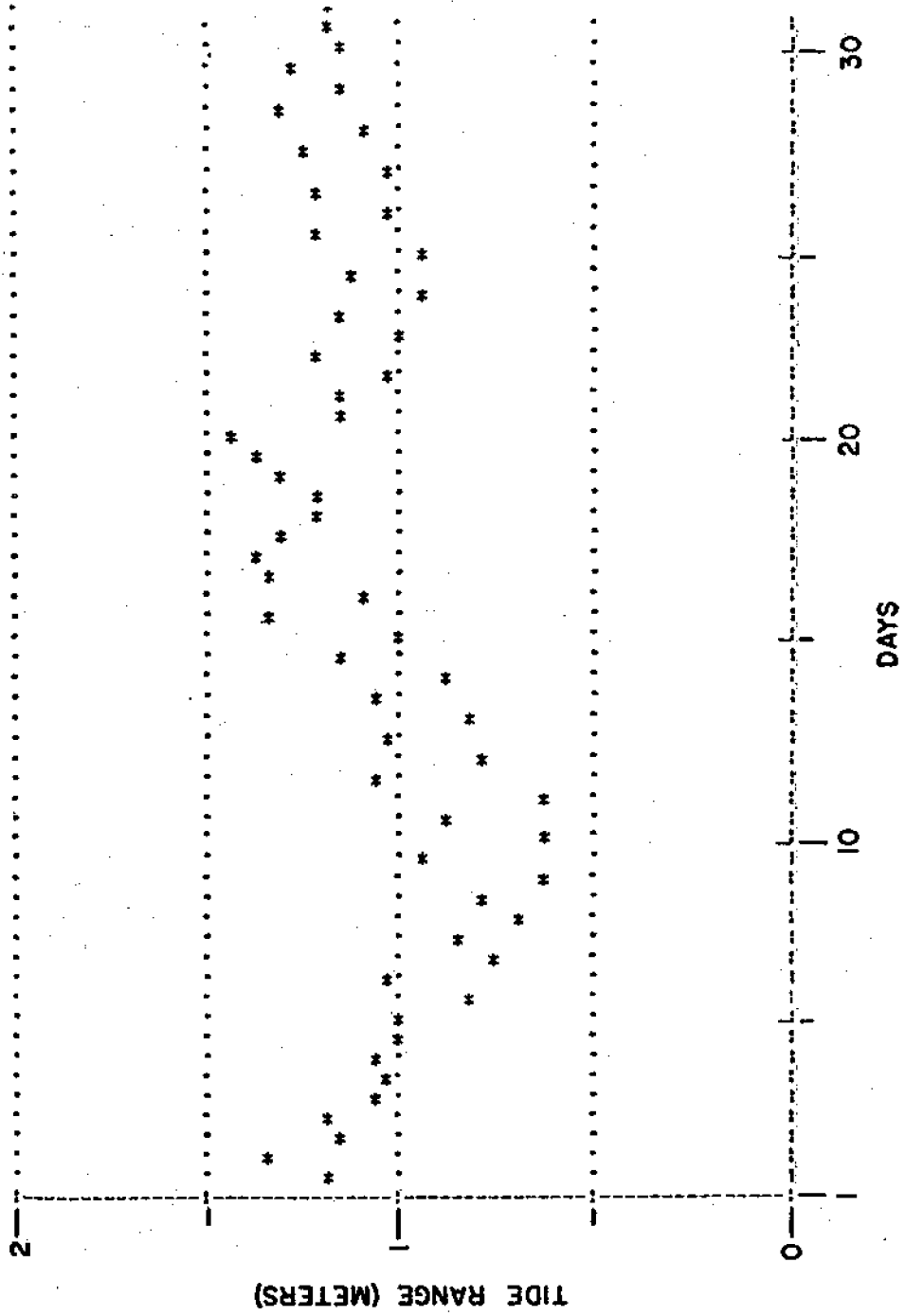


Figure 19. Time history of tide range - NC coast sample

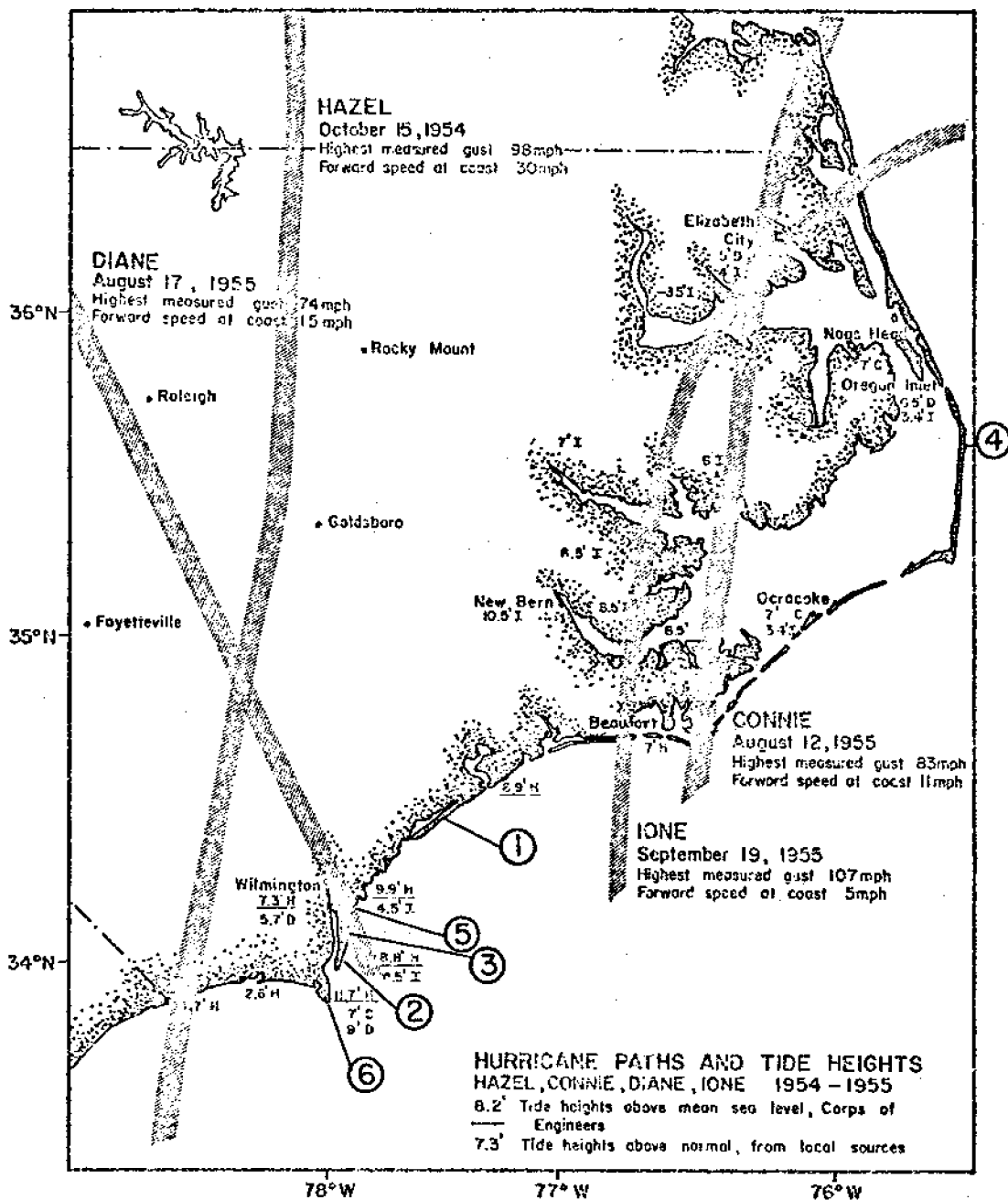


Figure 20. Hurricane paths and tide heights

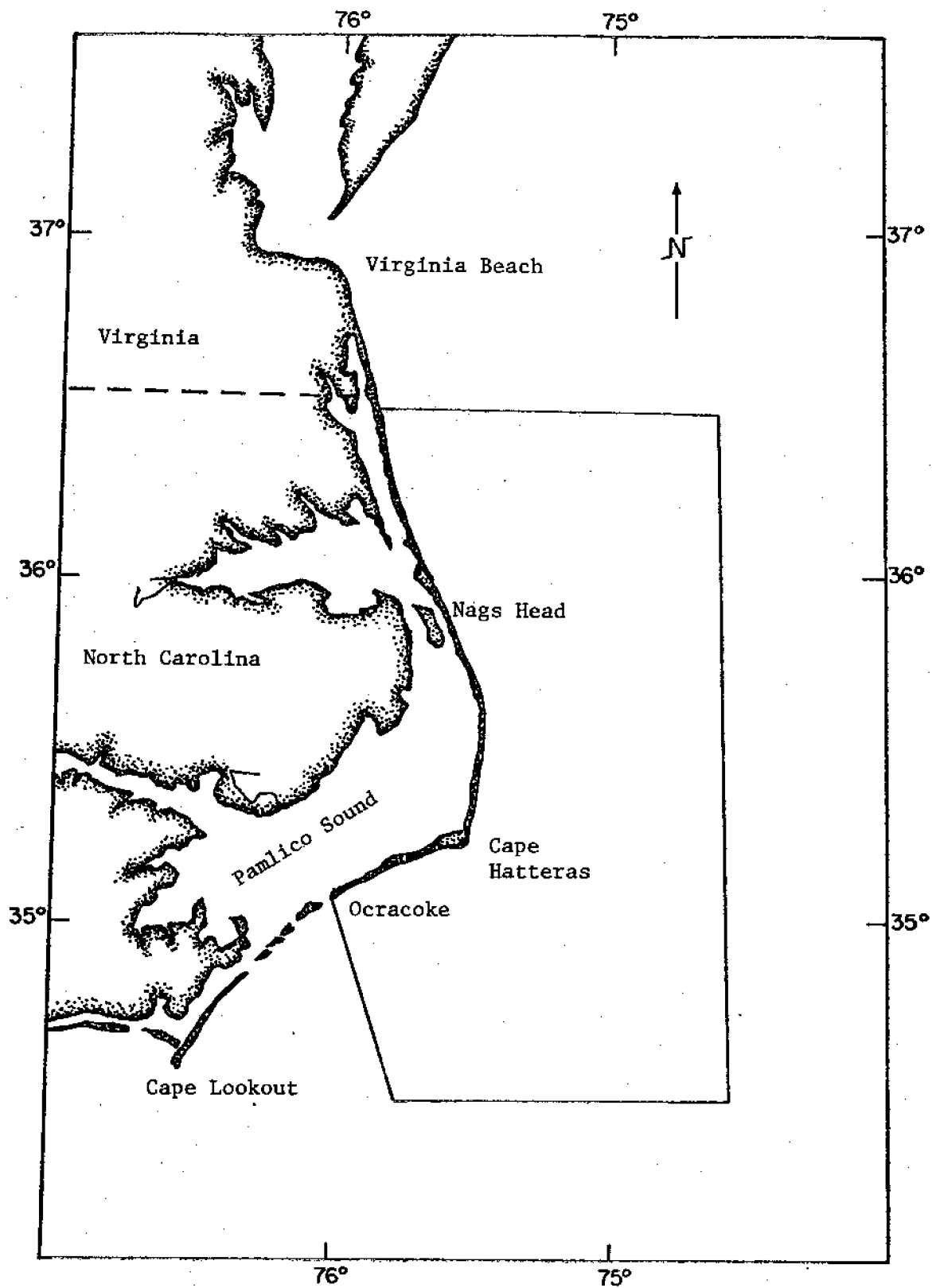


Figure 21. Offshore region east of Cape Hatteras

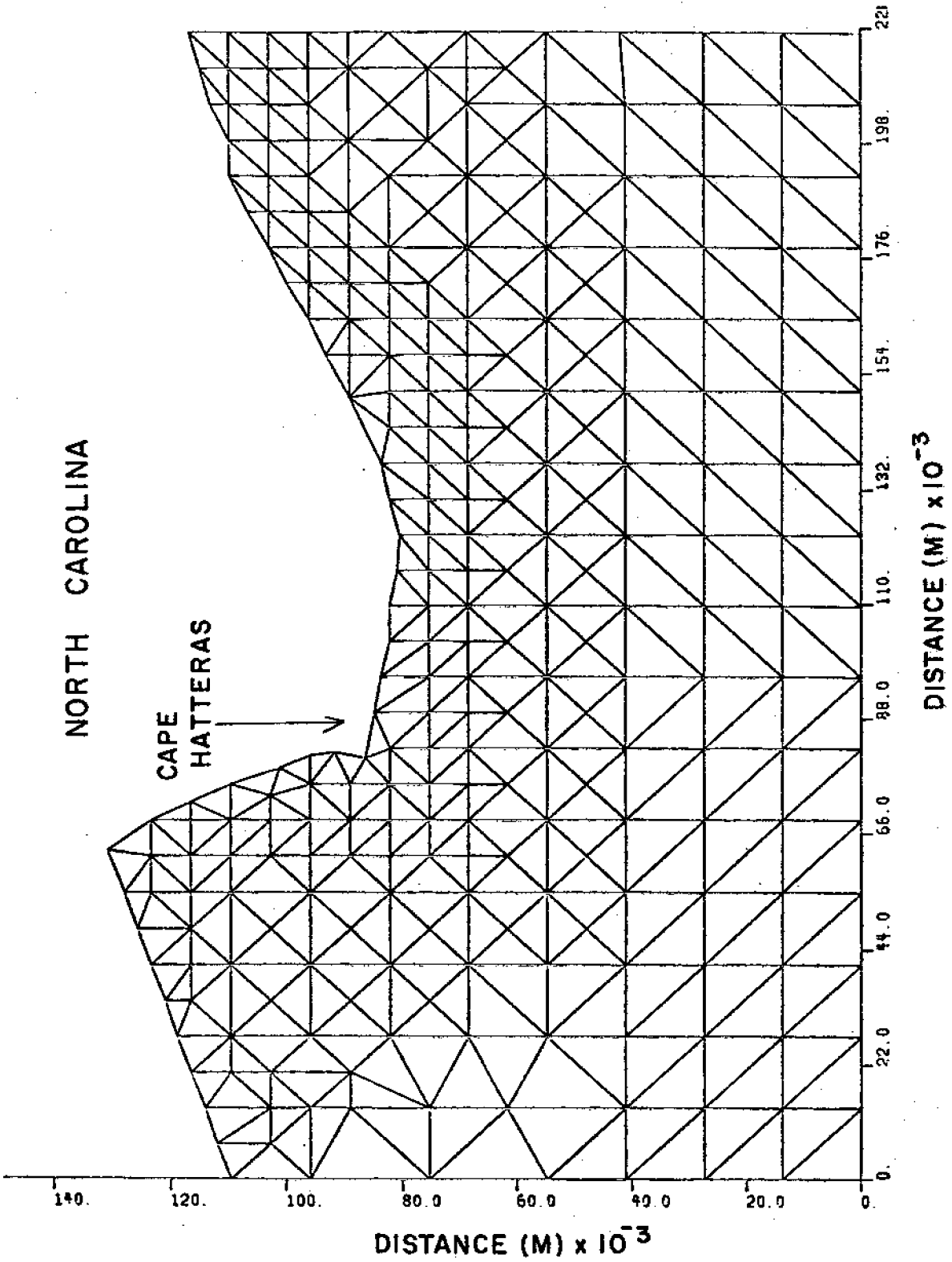


Figure 22. Discretization of the region east of Cape Hatteras



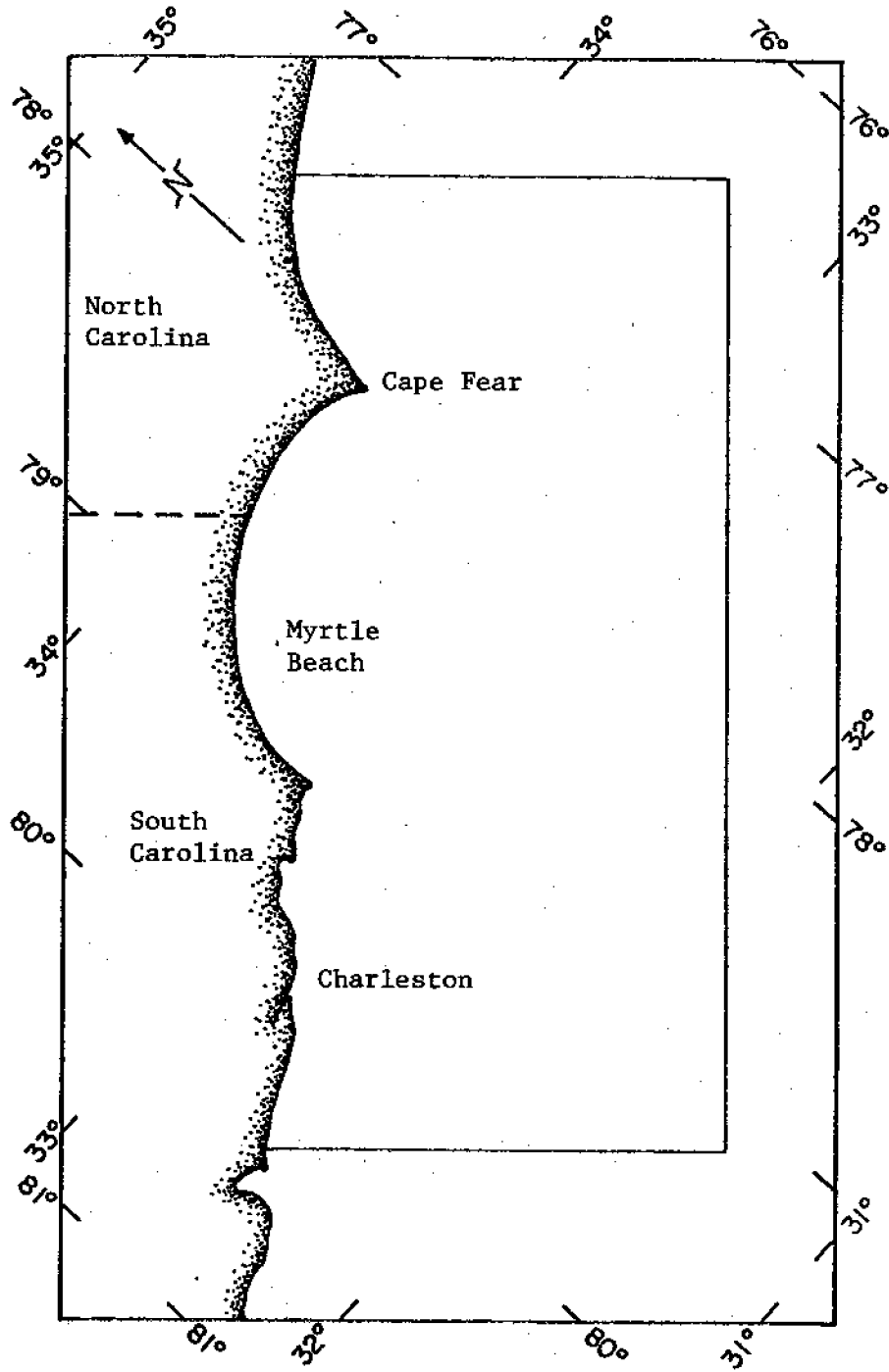


Figure 23. Offshore region south of Cape Hatteras

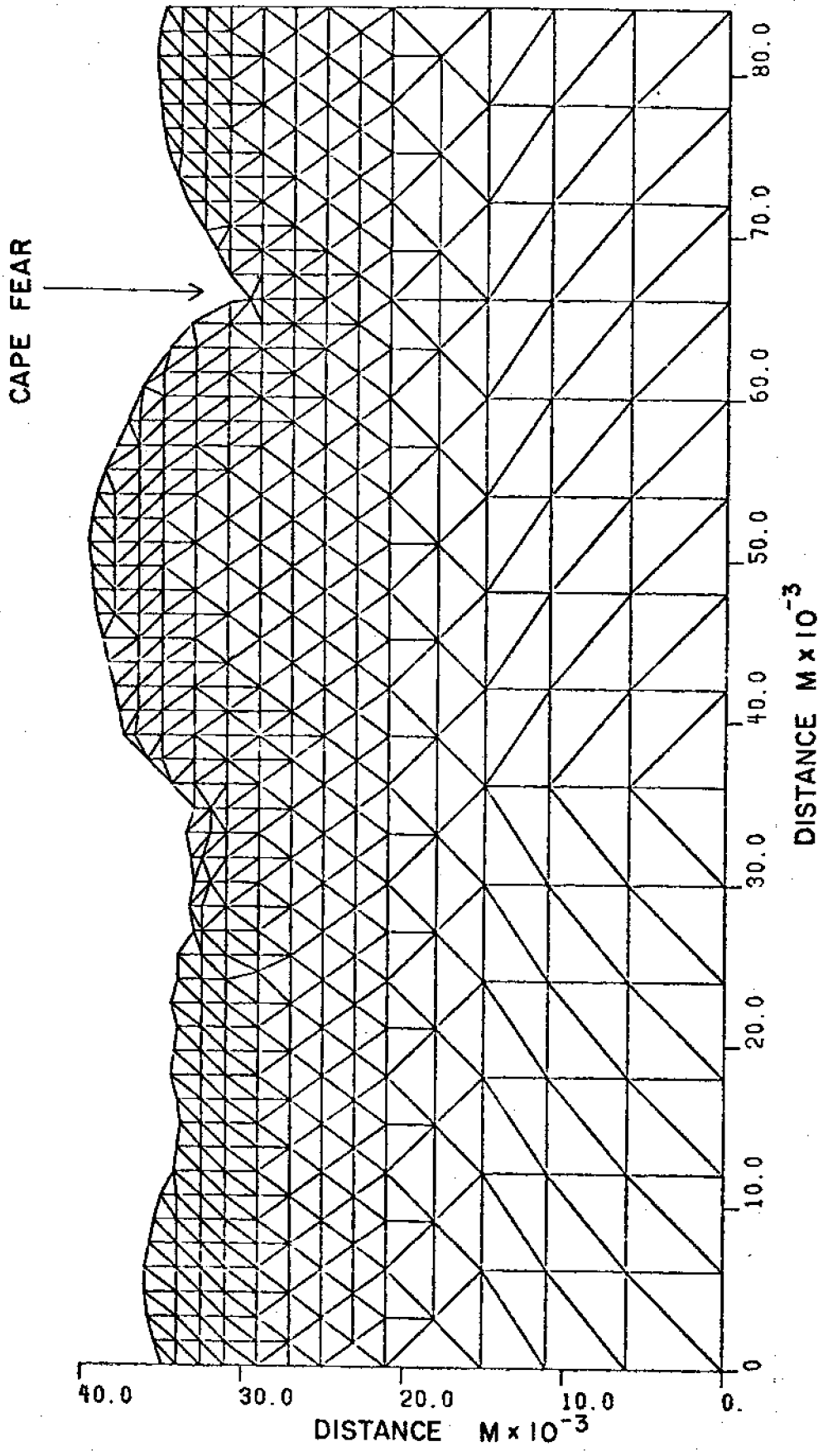


Figure 24. Discretization of the region south of Cape Hatteras

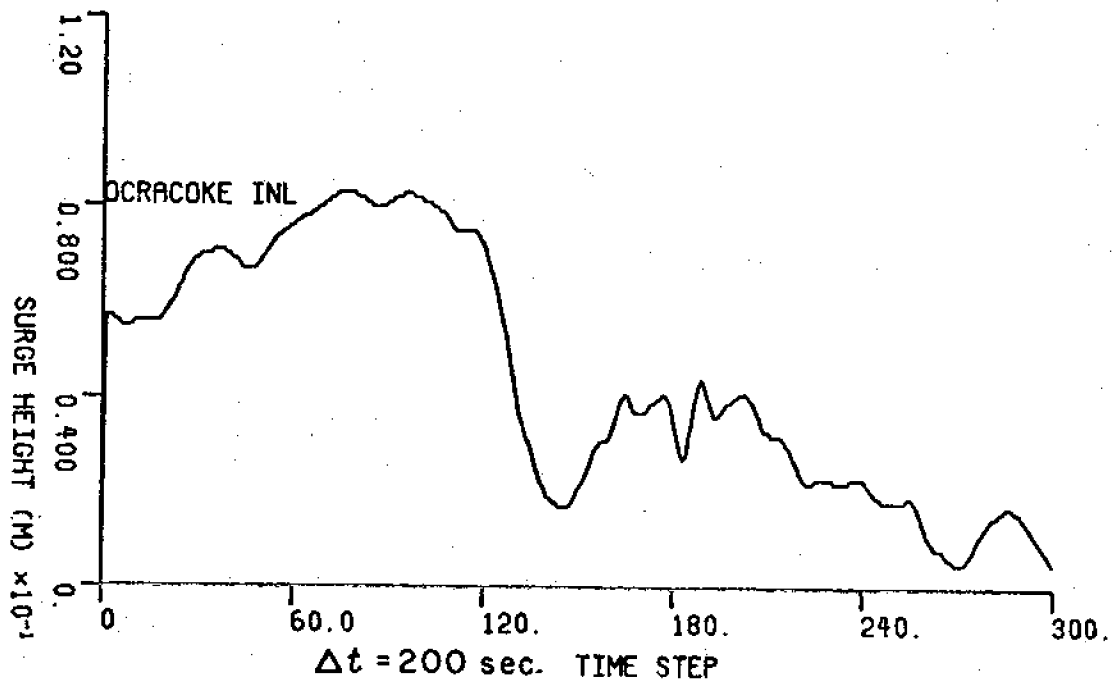


Figure 25 (a) . Storm tide -HZØ- Ocracoke

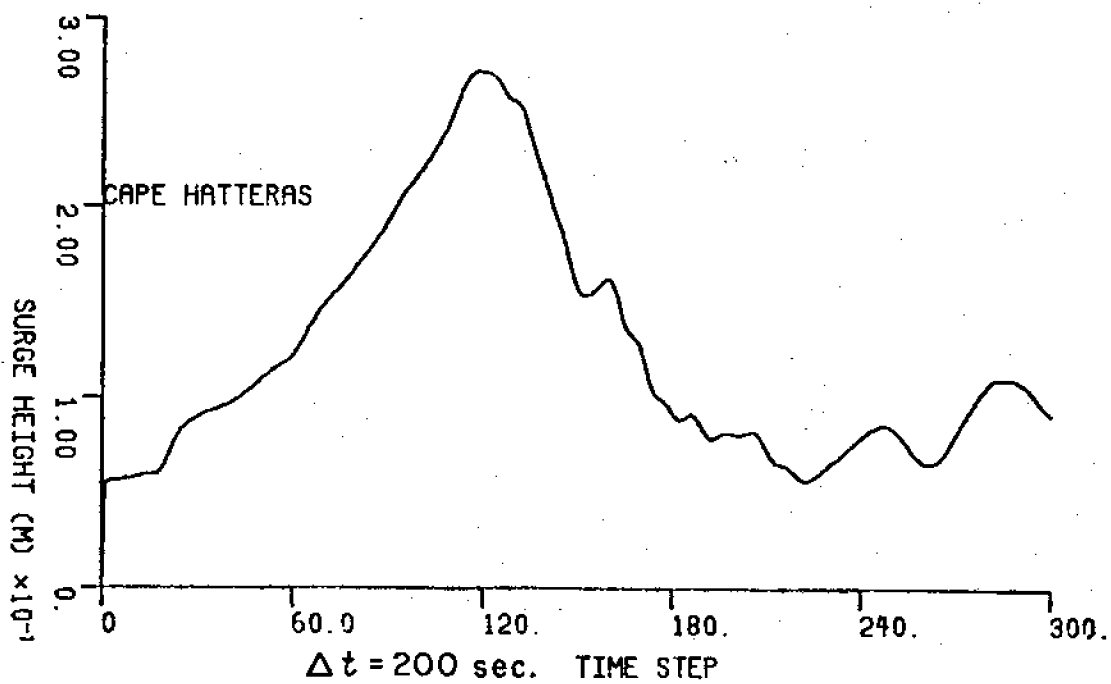


Figure 25 (b). Storm tide -HZ $\phi$ - Cape Hatteras

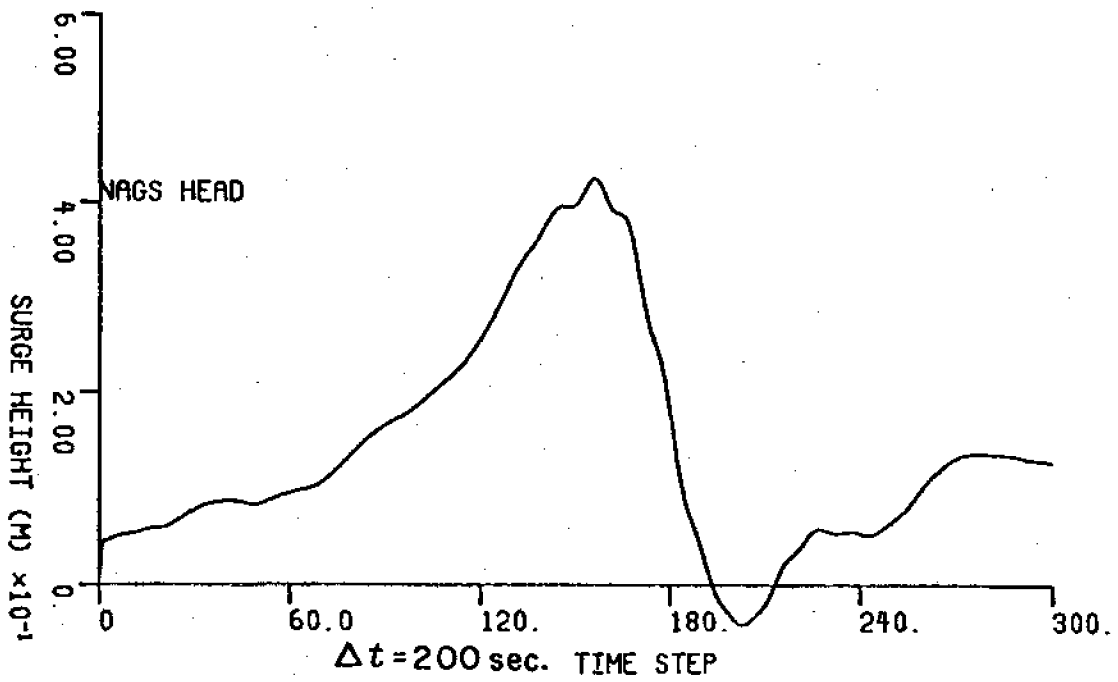


Figure 25 (c). Storm tide. -HZØ- Nags head

HURRICANE HZ1

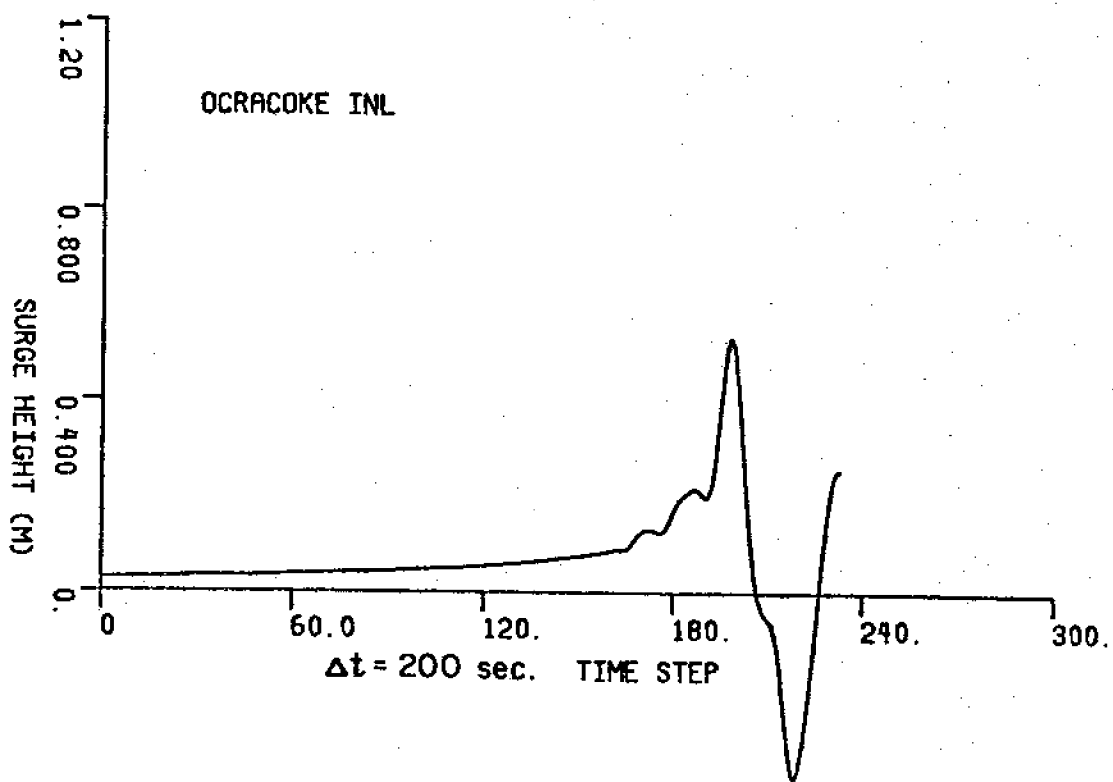


Figure 26 (a). Storm tide -HZ1- Ocracoke

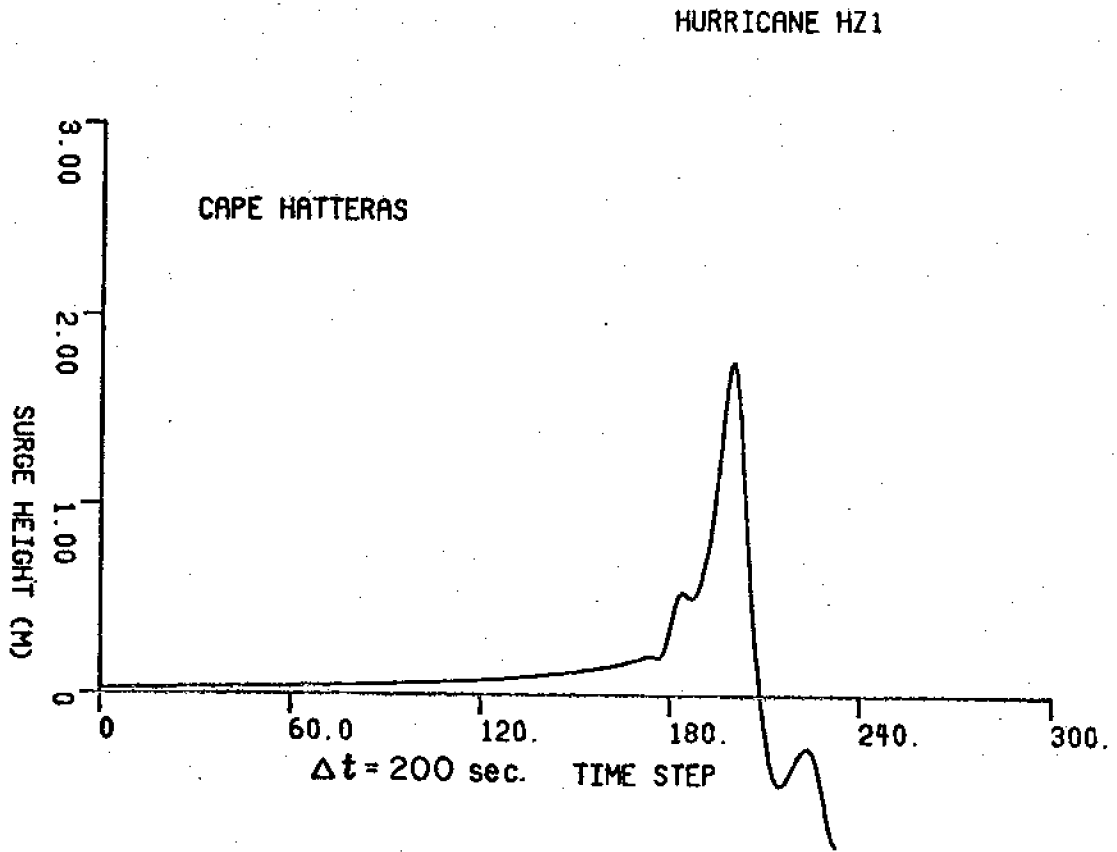


Figure 26(b). Storm tide -HZ1- Cape Hatteras

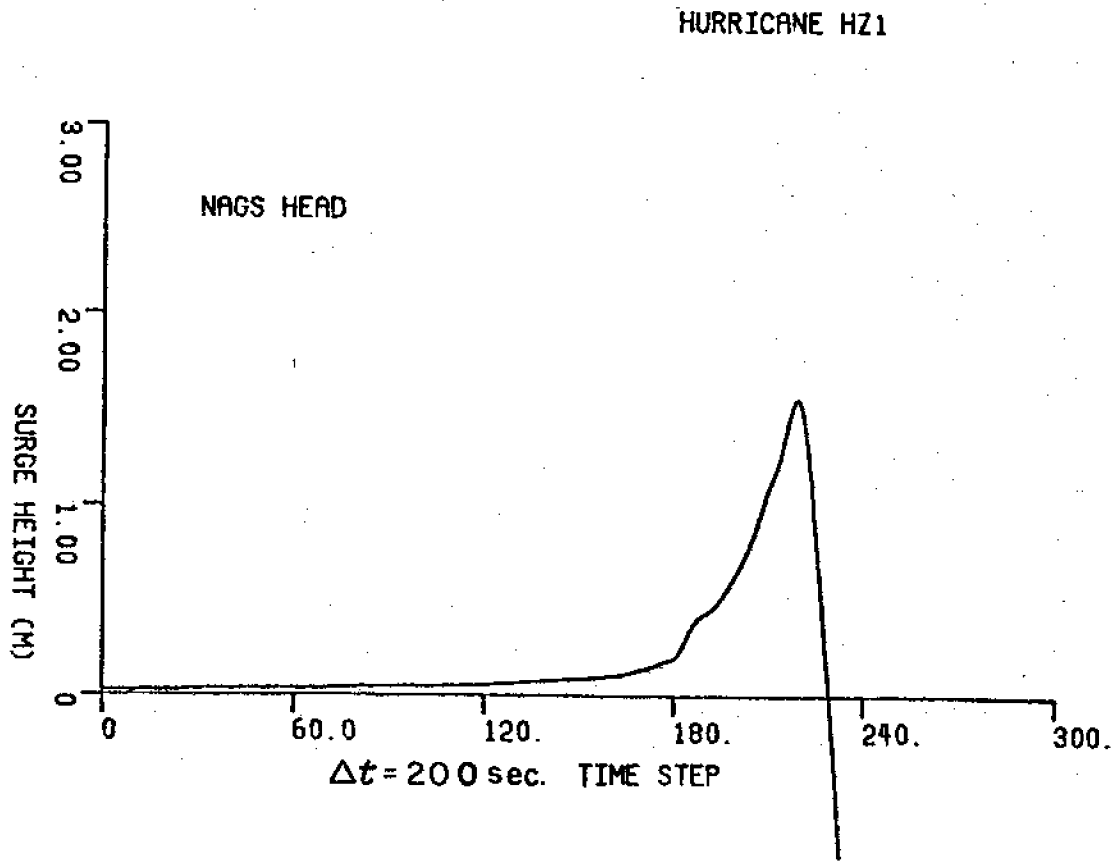


Figure 26 (c). Storm tide -HZ1- Nags Head



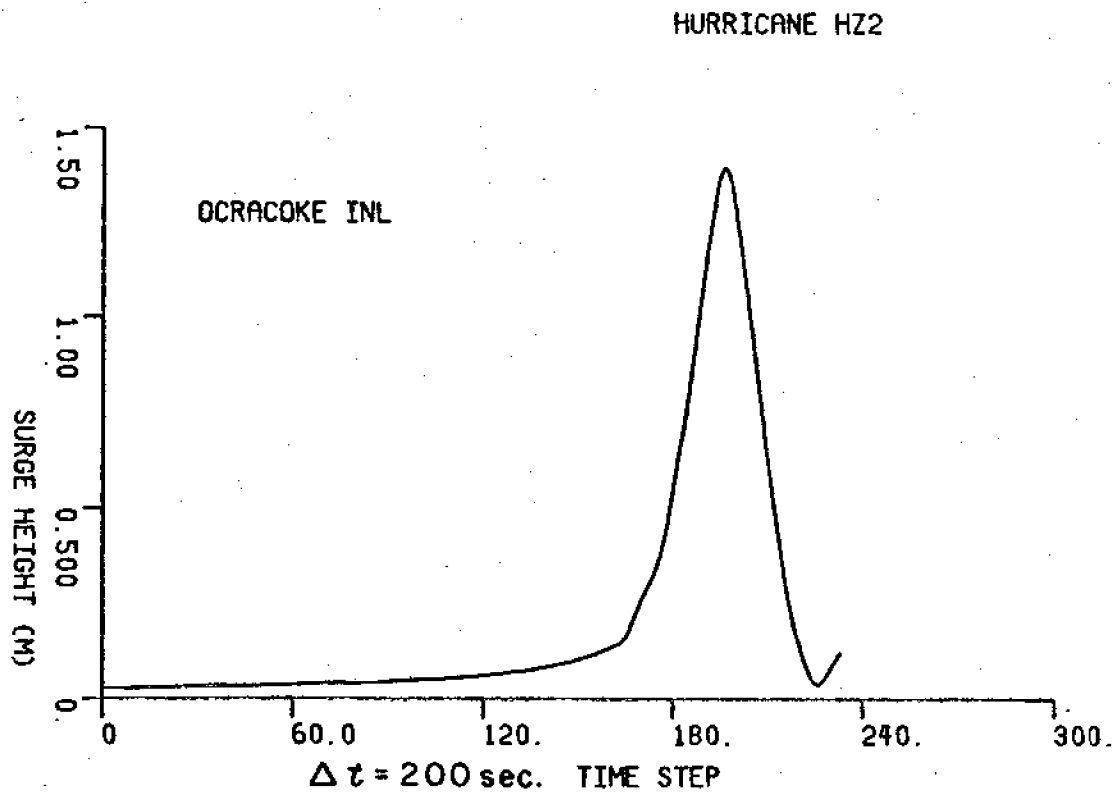


Figure 27(a). Storm tide -HZ2- Ocracoke

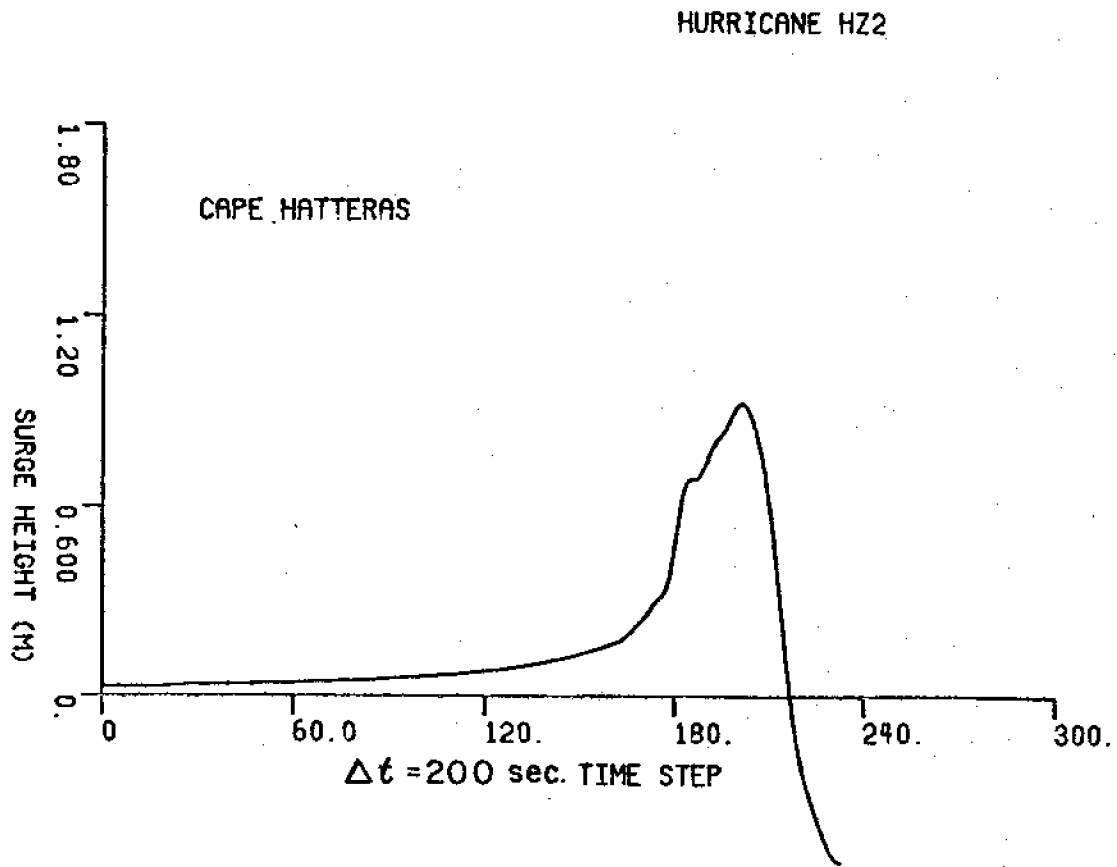


Figure 27 (b). Storm tide -HZ2- Cape Hatteras

HURRICANE HZ2

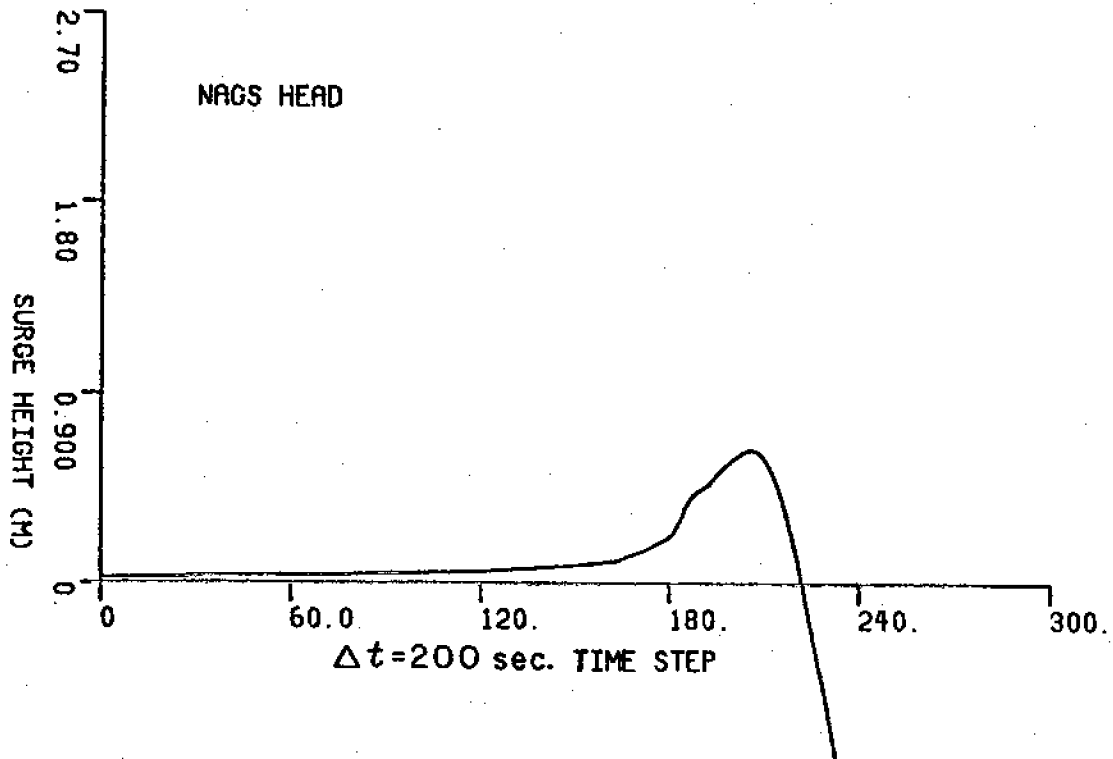


Figure 27(c). Storm tide -HZ2- Nags Head

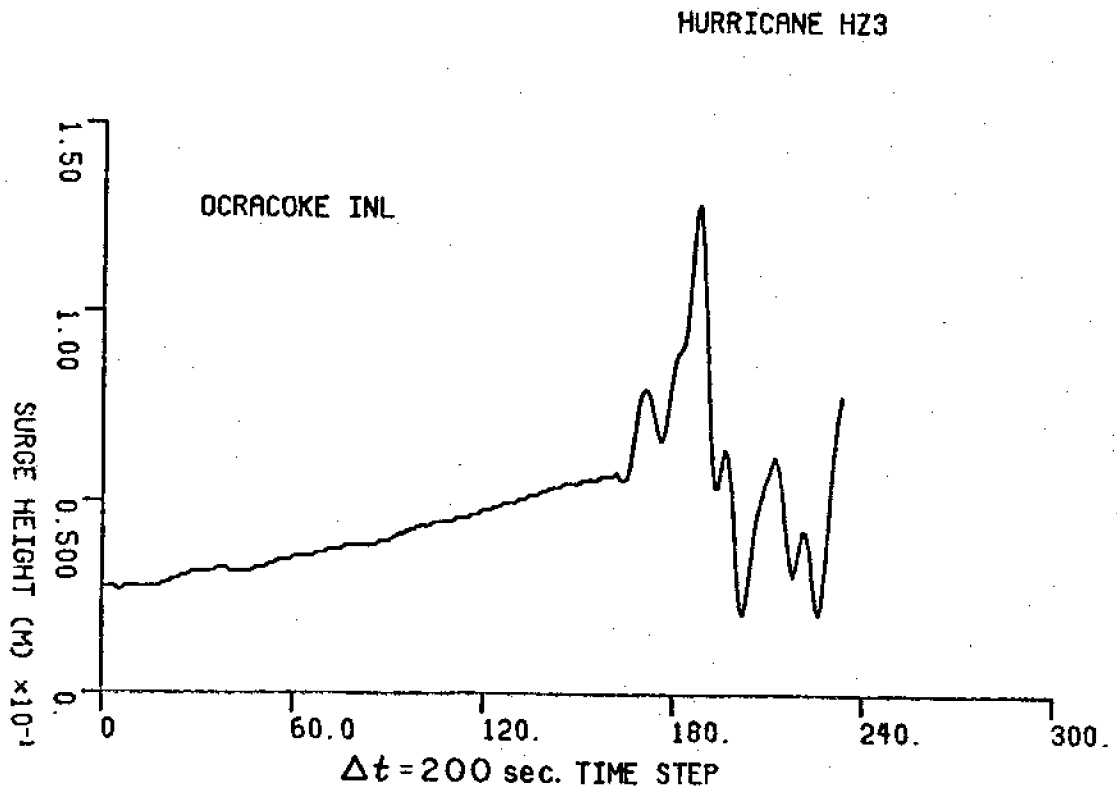


Figure 28 (a). Storm tide -HZ3- Ocracoke

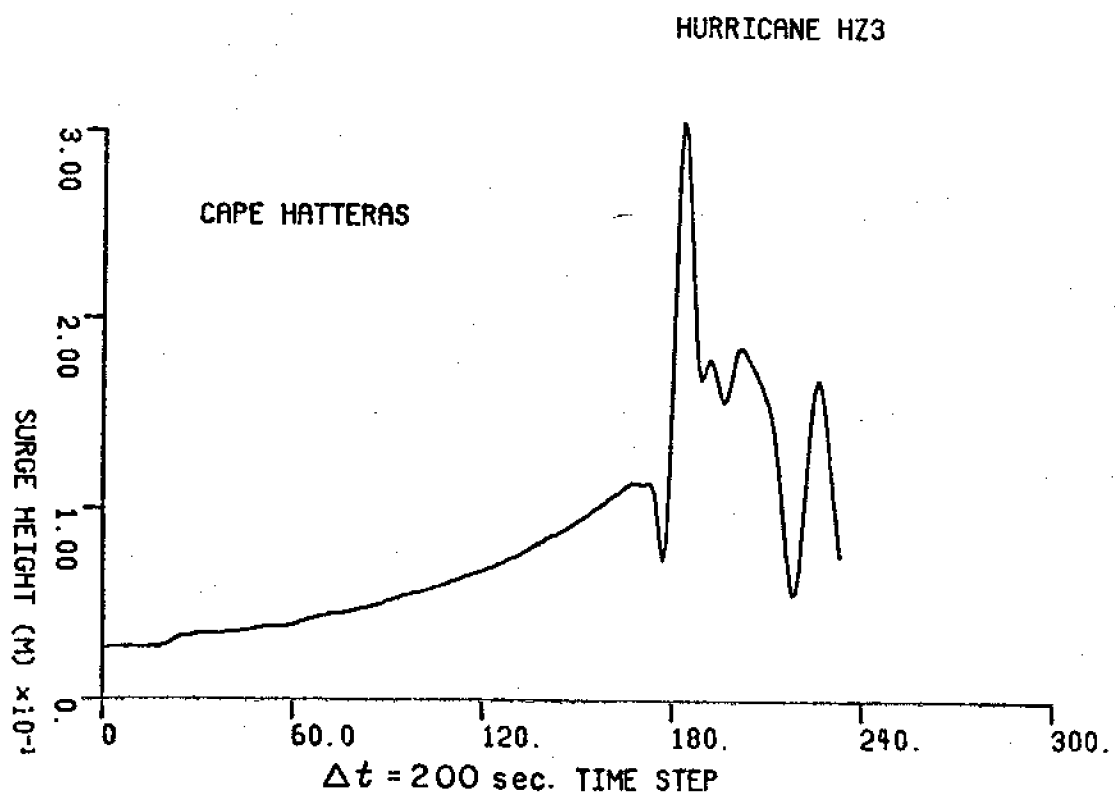


Figure 28(b). Storm tide -HZ3- Cape Hatteras

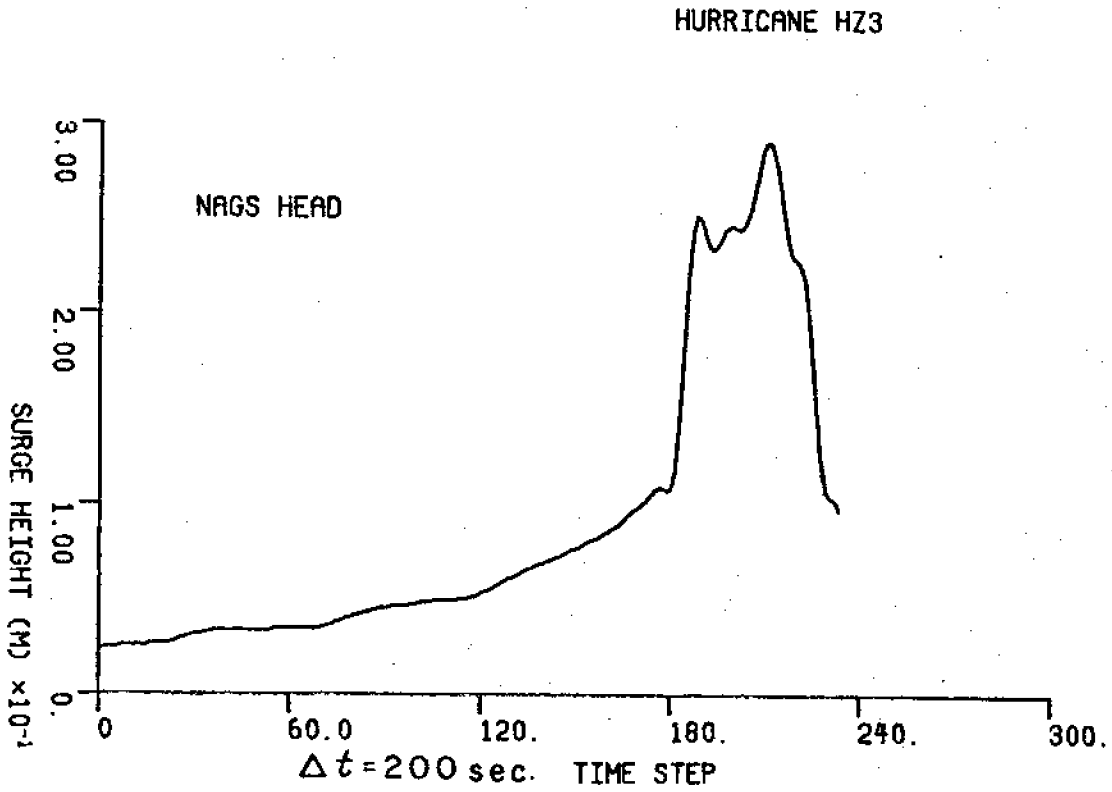
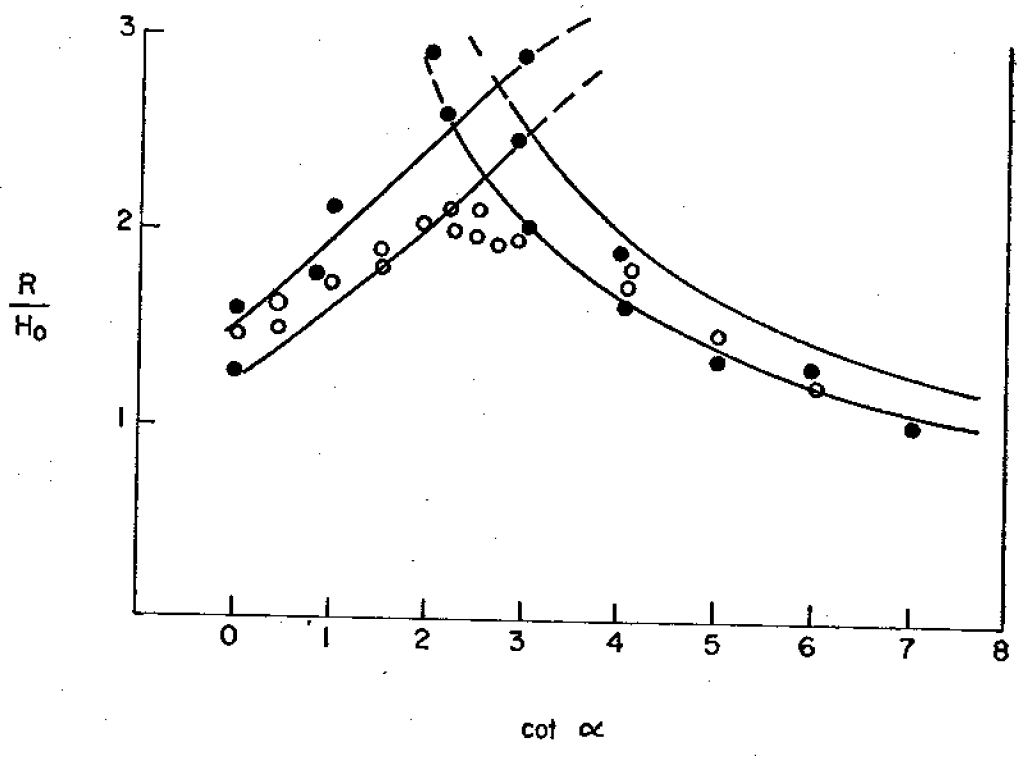


Figure 28 (c). Storm tide -HZ3- Nags Head



$H_0 / L_0 = 0.019$   
 $h / L_0 = 0.097$

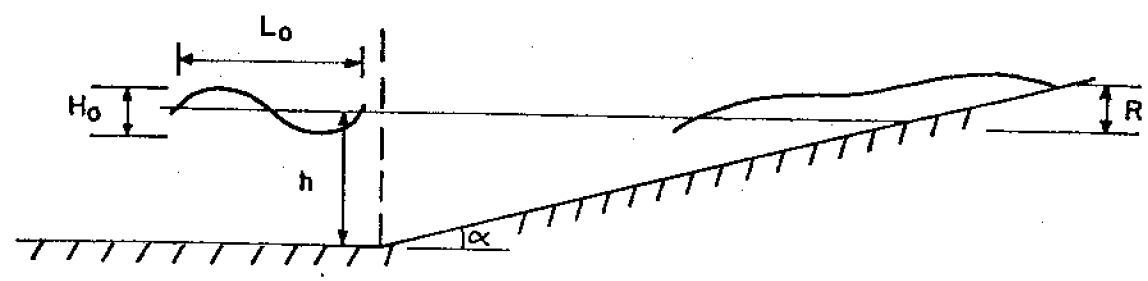


Figure 29. Experimental wave run-up (after Horikawa 1978)

## APPENDIX

## COMPUTER PROGRAM

A listing of the computer program used in this study is given in the following pages.



THIS PROGRAM COMPUTES THE SURGE ON LAND DUE TO WAVES RIDING OVER COASTAL WATERS WHOSE LEVELS HAVE BEEN ENHANCED BY STORM TIDE. THE TOTAL SURGE EFFECT IS THE SUM OF THE STORM TIDE AND THE WAVE SURGE. THIS EFFECT SHOULD BE TAKEN INTO EFFECT IN DECIDING ON THE SAFE SET-BACK LINE.

THE INPUT TO THIS PROGRAM ARE THE FIELD VALUES OF WAVE HEIGHT. THE DISTANCE FROM SHORE AT WHICH THE WAVE HEIGHT IS MEASURED, THE WAVE PERIOD, THE MEAN HIGH TIDE, THE STORM TIDE AND THE COEFFICIENTS OF THE CUBIC REGRESSION MODEL BY WHICH THE COASTAL PROFILE IS DEFINED. THE APPROACH IS BASED ON TRANSFORMING THE COASTAL PROFILE AND THE HYDRODYNAMICS TO THOSE OF A DISTORTED MODEL. THE WAVE STEEPNESS IS CONSIDERED AS THE PRIMARY FORCING FACTOR.

#### DEFINITION OF VARIABLES

MHT = MEAN HIGH TIDE  
 DO, D1, D2, D3 = THE FOUR COEFFICIENTS OF THE CUBIC REGRESSION MODEL FOR REPRESENTING THE COASTAL PROFILE:  $DEPTH = DO + D1 * X + D2 * X ** 2 + D3 * X ** 3$   
 DIST1 = THE PROTOTYPE DISTANCE FROM SHORELINE TO THE POINT WHERE THE DEPTH IS MEASURED AS DO.  
 HT = FIELD WAVE HEIGHT  
 T = FIELD WAVE PERIOD  
 STORMT = STORM TIDE IN THE REGION  
 COEF = FRICTION COEFFICIENT  
 IE = NO. OF ELEMENTS  
 DT = TIME STEP  
 SHDIST = DISTANCE FROM SHORE AT WHICH WAVE HEIGHT IS MEASURED  
 DM = INITIAL DEPTH IN THE MODEL; CHOOSE THIS PREFERABLY AROUND 2.5 METERS.  
 UL = ELEMENT LENGTH

DIMENSION U(32), Y(32), EL(15), UD(35), UDF(35),  
 1 UF(32), YF(32), F(4), FX(4), FXX(5,4), PXX(4),  
 2 BM(35), CU(32,7), CY(32,7), US(32), A(15,4,4), Z(15,4,4),  
 3 ED(35), EDF(35), XG(15,5), XGL(15,5), XGL2(15,5), XGL3(15,5),  
 4 W(15,5), AB(4,4), CC(2,3), CCU(32,7), CCY(32,7), XT(16),  
 5 H(15,5), SL(15,5), SECAL(15), SINAL(15), COSAL(15), RUP(3), XTOT(3)  
 DIMENSION CDSH(1)  
 COMMON /DISTC/ DO, D1, D2, D3  
 LOGICAL SOLIT, CHART, CHK1, CHK2  
 REAL MHT  
 DATA DO, D1, D2, D3, DIST1/12.57, -0.104500E-1, 0.208546E-4,  
 -0.115830E-7, 1575.0/  
 DATA HT, T, MHT, STORMT, COEF/4.0, 15.4, 0.79, 1.50, 0.05/  
 DATA SHDIST/600. /  
 DATA DM/2.0/  
 DO=11.37174187  
 D1=-0.00952488  
 D2=-5.8859513E-06

```

C4      D3=-4.0743861E-09
CC4     DIST1=1320.
CC1     DO=9.575
CC1     D1=-0.010885
CC1     D2=2.2629E-05
CC1     D3=-1.3092E-08
CC1     DIST1=1512.0
CC1     DO=10.6516
CC1     D1=0.002233
CC1     D2=-1.626E-04
CC1     D3=-9.1256E-10
CC1     DIST1=2088.
CC1     DO=12.00568
CC1     D1=-0.01034
CC1     D2=1.3843E-03
CC1     D3=-6.0386E-09
CC1     DIST1=1968.
CC1     DO=6.8011
CC1     D1=-0.01448
CC1     D2=-1.8729E-05
CC1     D3=-6.5606E-09
CC1     DIST1=2040.
CC3     DO=11.0835
CC3     D1=-0.00701
CC3     D2=1.06256E-03
CC3     D3=-5.1010E-09
CC3     DIST1=1944.
C       IE=3
C       DT=0.05
C       IE1=IE
C       NCP=5
C       NHB=3
C       FAC=1.2
C       COSH(X)=(EXP(X)+EXP(-X))/2.
C       G=9.81
C
C      COMPUTE THE INITIAL DEPTH AFTER ENHANCEMENT DUE TO ASTRONOMICAL
C      AND STORM TIDES
C
C      DO=DO+MHT+STORMT
C      CALL CDIST(D3,D2,D1,DO,DIST1,DIST)
C      XT(1)=DIST-SHDIST
C      UL=DM/O.3/IE
C      D=DO+D1*XT(1)+D2*XT(1)**2+D3*XT(1)**3
C      NHBPI=NHB+1
C      NHBMI=NHB-1
C      NFB=NHB*2+1
C      WRITE(3,111)
C 111  FORMAT(/T10,'STATION IDENTIFICATION'//)
C      WRITE(3,112) DO,D1,D2,D3,DIST1
C 112  FORMAT(/T5,'DO',F7.2,3X,'D1',E14.6,3X,'D2',E14.6,3X,'D3',
C      E14.6,3X,'INITIAL DISTANCE',F9.2,2X,'(M)')//)
C      WRITE(3,5) IE,UL,DT
C 5    FORMAT(/T5,'NO. OF ELEMENTS',3X,I3,8X,'ELE. LENGTH',3X,F5.1,
C      1 2X,'M',8X,'TIME STEP',3X,F6.3,2X,'SEC')//)
C      WRITE(3,6) D,HT,MHT
C      WRITE(3,8) T
C
C      COMPUTE THE PROTOTYPE WAVE LENGTH.
C
C      WL=G*T**2/6.28
C 121  WL=WL-0.2
C      WL2=G*T**2/6.28*TANH(6.28*D/WL)
C      IF(ABS(WL2-WL).LT.0.2) GO TO 122
C      GO TO 121
C 122  T=SQRT(60./TANH(6.28*DO/60.))*6.28/G)
C 122  WLM=DM/D*WL
C      HT=HT*WLM/WL
C      T=SQRT(WLM/TANH(6.28*DM/WLM))*6.28/G)
C 6    FORMAT(/T5,'DEPTH',2X,F5.2,2X,'M',8X,'HAVE HEIGHT',F5.2,2X,
C      1  'M',10X,'MEAN HIGH TIDE',F5.2,2X,'M')//)
C 8    FORMAT(/T10,'PERIOD',F4.1,2X,'SEC')//)
C 177  FORMAT(/T6,'TIME',T20,'WATER LEVELS (M) AT THE NODES W.R.T.',
C      1  ' STILL WATER LEVEL')
C
C      COMPUTE THE MODEL SCALES.
C
C      XS=DM/O.3/SHDIST
C      YS=DM/D

```

```

C      WRITE(3,120) XS,YS
120   FORMAT(/T10,'HORIZONTAL SCALE ',F6.3,10X,'VERTICAL SCALE ',F6.3/)
C      HT=HT*20.*DM/WL
      WRITE(3,135) HT,T
135   FORMAT(/T10,'MODEL WAVE HEIGHT =',F5.2,2X,'M',10X,'MODEL WAVE',
1     ' PERIOD =',F6.2,2X,'SEC'/)
      SH=SHDIST*XS
      WRITE(3,137) DM,SH
137   FORMAT(/T10,'MODEL INITIAL DEPTH =',F6.2,2X,'M',10X,
1     ' MODEL SHORE DISTANCE =',F8.2,2X,'M'////)
C      TRANSFORM THE REGRESSION COEFFICIENTS TO THOSE OF THE MODEL.
C
      D=DM
      DO=DO*YS
      D1=D1*YS/XS
      D2=D2*YS/XS**2
      D3=D3*YS/XS**3
      XT(I)=XT(I)*XS
      DIST1=DIST1*XS
C
      WRITE(3,177)
      IEM1=IE-1
      DO 15 I=1,IE
15    EL(I)=UL
      EL150=UL*FAC
      DTH=DT*0.5
      NT=2*IE+2
      NTP3=NT+3
      NTM1=NT-1
      NTM2=NT-2
      NTM3=NT-3
      NTM4=NT-4
      NTM5=NT-5
3000  DO 3000 I=2,IE
      XT(I)=XT(I-1)+EL(I-1)
      DO 10 I=1,IEM1
      CALL SPINT(XG,XGL,XGL2,XGL3,IE,EL,W,NGP,I)
      CALL SOXL(XG,EL,IE,NGP,XGL,XGL2,XGL3,I)
      CALL SHSL(H,SL,XG,I,XT)
      SECAL(I)=SQRT(1.+SL(I,3)**2)
      SINAI(I)=-SL(I,3)/SECAL(I)
      COSAI(I)=1./SECAL(I)
10    CONTINUE
      DO 30 N=1,NTP3
      U(N)=0.00001
      Y(N)=0.0
      UD(N)=0.
      ED(N)=0.
30    DO 32 I=2,NTP3,2
32    U(I)=0.
      DO 33 I=1,3
      RUP(I)=0.
33    XTOT(I)=0.
      KN=1
      SIG=6.28/T
      AMP=HT/2.
      DO 35 I=1,NT
      DO 35 J=1,NFB
      CU(I,J)=0.
35    CY(I,J)=0.
      DO 37 I=1,IEM1
      CALL QELCS(A,F,NGP,W,XG,XGL,XGL2,XGL3,EL,IE,I)
37    CONTINUE
      DO 38 J1=1,2
      DO 38 J2=1,2
38    AB(J1,J2)=A(IEM1,J1+2,J2+2)
      CALL SOC(A,CY,IE,NT,NFB,1,IEM1)
      CALL REST1S(CC,CY,NTM3,NTM2)
      CD1=CX(2,3)
      CD2=CX(3,2)
      CD3=CX(4,1)
      DO 61 J=5,7
      CY(I,J)=0.
61    CONTINUE
      DO 62 J=2,4
      K=5-J
      CY(J,K)=0.
62    CONTINUE

```

```

CY(1,4)=1.
DO 68 I=1,NT
DO 68 J=1,7
68 CCY(I,J)=CY(I,J)
CALL SPBAND(NT,NHB,NHBP1,NHBM1,NFB,CY,2,NTM4)
CALL SPINT(XG,XGL,XGL2,XGL3,IE,EL,W,NGP,IE)
CALL SGXL(XG,EL,IE,NGP,XGL,XGL2,XGL3,IE)
CALL SHSL(H,SL,XG,IE,XT)
IND=0
TIME=0.
DO 1000 JKN=1,500
TIME=JKN*DT
SIGT=SIG*TIME
Y1=AMP*SIN(SIGT)
YD1=AMP*SIG*COS(SIGT)
DO 42 N=1,NT
UF(N)=U(N)
YF(N)=Y(N)
UDF(N)=UD(N)
42 EDF(N)=ED(N)
C
IF(EL(IE).LT.EL150) GO TO 704
CALL SGENW(IND,U,Y,H,EL,IE,NT,NTM1,NTM2,NTM3,NTM5,CC,UL,
1 NTP3,SL,NGP,W,A,AB,CY,UD,ED,NFB,XG,XGL,XGL2,XGL3,CCY,XT)
DO 43 N=NTM3,NT
UF(N)=U(N)
YF(N)=Y(N)
UDF(N)=UD(N)
43 EDF(N)=ED(N)
DO 44 N1=NTM1,NT
DO 44 N2=1,7
CU(N1,N2)=0.
CY(N1,N2)=0.
44 CCY(N1,N2)=0.
704 NA=0
ACC1=UDF(NTM1)+UF(NTM1)*UF(NT)
EL1=EL(IE)
ED(1)=YD1
714 NA=NA+1
DO 440 I1=1,NT
DO 440 I2=1,7
440 CU(I1,I2)=0.
ACC2=UD(NTM1)+U(NTM1)*U(NT)
ACCM=(ACC1+ACC2)/2.
S=UF(NTM1)*DT+0.3*ACCM*DT*DT
EL(IE)=EL1+S
U(NTM1)=UF(NTM1)+ACCM*DT
Y(NTM1)=YF(NTM1)-S*SL(IE,5)
CALL SPINT(XG,XGL,XGL2,XGL3,IE,EL,W,NGP,IE)
CALL SGXL(XG,EL,IE,NGP,XGL,XGL2,XGL3,IE)
CALL SHSL(H,SL,XG,IE,XT)
SECAL(IE)=SQRT(1.+SL(IE,3)**2)
SINAL(IE)=-SL(IE,3)/SECAL(IE)
COSAL(IE)=1./SECAL(IE)
CALL GELCS(A,F,NGP,W,XG,XGL,XGL2,XGL3,EL,IE,IE)
DO 450 J1=1,2
DO 450 J2=1,2
450 A(IE,J1,J2)=AB(J1,J2)+A(IE,J1,J2)
CALL REST2S(CC,CY,NTM3,NTM2)
K1=2*IE-1
K4=K1+3
M1=0
DO 75 N1=K1,K4
M1=M1+1
LL=4-M1
DO 75 N2=1,4
L=LL+N2
CY(N1,L)=A(IE,M1,N2)
75 CCY(N1,L)=CY(N1,L)
CALL GELCUS(Z,F,NGP,W,XG,XGL,XGL2,XGL3,EL,IE,Y,H,DHDX,SL)
CALL SGC(Z,CU,IE,NT,NFB,1,IE)
DO 77 I=1,NT
DO 77 J=1,7
77 CCU(I,J)=CU(I,J)
IF(IND.EQ.1) IB=NTM5
IF(IND.EQ.0) IB=NTM3
CALL SPBAND(NT,NHB,NHBP1,NHBM1,NFB,CU,2,NT)
CALL SPBAND(NT,NHB,NHBP1,NHBM1,NFB,CY,IB,NT)
IND=0
CALL SGBMU(NT,IE,XG,XGL,XGL2,XGL3,BM,U,Y,H,NGP,W,EL,NTP3,

```

```

1  FRICSG, O, SECAL, SINAL, COSAL, COEF, SL)
CALL BANDS1(NT, NHB, NHBP1, NHBM1, NFB, CU, BM, UD, CCU, NTP3)
CALL SOBMY(NT, IE, XG, XGL, XGL2, XGL3, BM, U, Y, H, NOP, W, EL, NTP3, SL)
BM(2)=BM(2)-ED(1)*CD1
BM(3)=BM(3)-ED(1)*CD2
BM(4)=BM(4)-ED(1)*CD3
BM(1)=ED(1)
CALL BANDS1(NT, NHB, NHBP1, NHBM1, NFB, CY, BM, ED, CCY, NTP3)
DO 80 N=2,NTM2
U(N)=UF(N)+(UD(N)+UDF(N))*DTH
80 Y(N)=YF(N)+(ED(N)+EDF(N))*DTH
Y(1)=Y1
U(1)=UF(1)+(UDF(1)+UD(1))*DTH
Y(NT)=YF(NT)+(ED(NT)+EDF(NT))*DTH
U(NT)=UF(NT)+(UDF(NT)+UD(NT))*DTH
IF(NA. EQ. 1) GO TO 100
DO 90 N=1,NTM1
IF((ABS(US(N)/U(N))-1.). GT. 0.1) GO TO 100
90 CONTINUE
GO TO 110
100 DO 105 N=1,NTM1
105 US(N)=U(N)
GO TO 714
110 RUP(1)=RUP(2)
RUP(2)=RUP(3)
RUP(3)=Y(NTM1)
XTOT(1)=XTOT(2)
XTOT(2)=XTOT(3)
XTOT(3)=(XT(IE)+EL(IE))/XS-DIST
WRITE(3,176) TIME, (Y(I), I=1,NT,2)
C WRITE(10,176) TIME, (Y(I), I=1,NT,2)
CHK1=RUP(1).GT.RUP(2).AND.RUP(2).GT.RUP(3).AND.IE.GT.IE1
IF(.NOT.CHK1) GO TO 155
XTT=XTOT(1)
RP=RUP(1)
GO TO 160
155 CHK2=(ABS(Y(3)).GE.4.0. OR. ABS(Y(3)).GE.4.0)
IF(.NOT.CHK2) GO TO 1000
XTT=XTOT(3)
RP=RUP(3)
160 WRITE(3,174) RP
174 FORMAT(/T10, 'MAXIMUM RUN-UP ON THE MODEL =',F7.3,2X, 'M')
WRITE(3,183)
PRP=RP/YS
WRITE(3,179) PRP
176 FORMAT(/T2,FB,2,5X,14FB,3)
178 FORMAT(/T20, 'LAND INTRUSION DISTANCE DUE TO WAVE ATTACK =',F10.3,
1 2X, 'M')
179 FORMAT(/T10, 'PROTOTYPE SURGE HEIGHT DUE TO WAVE ATTACK =',F7.3,
1 2X, 'M')
181 FORMAT(/T10, 'LAND INTRUSION DISTANCE (FROM MEAN LOW WATER',
1  MARK) DUE TO STORM TIDE AND WAVE ATTACK =',F10.2,2X, 'M')
180 FORMAT(/T10, 'LAND INTRUSION DISTANCE (FROM MEAN LOW WATER MARK)',
1  DUE TO STORM TIDE =',F10.2,2X, 'M')
182 FORMAT(/T10, 'TOTAL STORM SURGE (STORM TIDE + WAVE ATTACK) =',F6.2,
1 2X, 'M')
183 FORMAT(/T10, 'MAXIMUM RUN-UP ON THE MODEL DIVIDED BY THE VERTICAL',
1  SCALE GIVES THE PROTOTYPE SURGE HEIGHT')
WRITE(3,184) STORMT
184 FORMAT(/T10, 'STORM TIDE FOR THIS STATION =',F6.2,2X, 'M')
SUR=PRP+STORMT
WRITE(3,182) SUR
XTOT1=DIST-DIST1/XS
WRITE(3,178) XTT
WRITE(3,180) XTOT1
XTOT2=XTT+XTOT1
WRITE(3,181) XTOT2
STOP
1000 CONTINUE
STOP
END
SUBROUTINE SFN(X, XL, XL2, XL3, EL, I, F, IE)
C DIMENSION F(4), EL(15)
F(1)=1.-3.*XL2+2.*XL3
F(2)=X+EL(I)*(XL3-2.*XL2)
F(3)=3.*XL2-2.*XL3
F(4)=EL(I)*(XL3-XL2)
RETURN
END

```

```

C      SUBROUTINE SFXN(XL, XL2, EL, I, FX, IE)
      DIMENSION FX(4), EL(15)
      FX(1)=6. *(XL2-XL)/EL(I)
      FX(2)=1. -4. *XL+3. *XL2
      FX(3)=6. *(XL-XL2)/EL(I)
      FX(4)=3. *XL2-2. *XL
      RETURN
      END
C      SUBROUTINE SFXX(X, EL, I, PXX, IE)
      DIMENSION EL(15), PXX(4)
      PXX(1)=-6. /(EL(I)*EL(I))+12. *X/(EL(I)*EL(I)*EL(I))
      PXX(2)=-4. /EL(I)+6. *X/EL(I)*EL(I)
      PXX(3)=6. /(EL(I)*EL(I))-12. *X/EL(I)*EL(I)*EL(I)
      PXX(4)=6. *X/EL(I)*EL(I)-2. /EL(I)
      RETURN
      END
C      SUBROUTINE SGC(A, C, IE, N, NFB, IB, IEND)
      DIMENSION A(15, 4, 4), C(32, 7)
      DO 100 I=IB, IEND
      K1=2*I-1
      K4=K1+3
      M1=0
      DO 75 N1=K1, K4
      M1=M1+1
      LL=4-M1
      DO 75 N2=1, 4
      L=LL+N2
75 C(N1, L)=C(N1, L)+A(I, M1, N2)
100 CONTINUE
      RETURN
      END
C      SUBROUTINE GELCS(A, F, NGP, W, XG, XGL, XGL2, XGL3, EL, IE, I)
      DIMENSION A(15, 4, 4), W(15, 5), FGP(5), EL(15), XG(15, 5),
1 XGL(15, 5), XGL2(15, 5), XGL3(15, 5), FGP1(5, 4), F(4)
      DO 10 K=1, NGP
      X=XG(I, K)
      XL=XGL(I, K)
      XL2=XGL2(I, K)
      XL3=XGL3(I, K)
      CALL SFXN(X, XL, XL2, XL3, EL, I, F, IE)
      DO 10 L=1, 4
10 FGP1(K, L)=F(L)
      DO 18 K1=1, 4
      DO 18 K2=1, 4
      DO 15 K=1, NGP
15 FGP(K)=FGP1(K, K1)*FGP1(K, K2)
      CALL SGINT(FGP, NGP, W, I, IE, FINT)
      A(I, K1, K2)=FINT
18 CONTINUE
      RETURN
      END
C      SUBROUTINE GELCUS(A, F, NGP, W, XG, XGL, XGL2, XGL3, EL, IE, Y, H, DHDX, SL)
      DIMENSION A(15, 4, 4), W(15, 5), FGP(5), EL(15), XG(15, 5), XGL(15, 5),
1 XGL2(15, 5), XGL3(15, 5), FGP1(5, 4), F(4), Y(32), H(15, 5), FX(4),
2 FGP2(5, 4), SL(15, 5)
      DO 20 I=1, IE
      M1=2*I-1
      M2=M1+1
      M3=M2+1
      M4=M3+1
      DO 12 K=1, NGP
      X=XG(I, K)
      XL=XGL(I, K)
      XL2=XGL2(I, K)
      XL3=XGL3(I, K)
      CALL SFXN(X, XL, XL2, XL3, EL, I, F, IE)
      CALL SFXN(XL, XL2, EL, I, FX, IE)
      G1=TP(F(1), Y(M1), F(2), Y(M2), F(3), Y(M3), F(4), Y(M4))
      G2=TP(FX(1), Y(M1), FX(2), Y(M2), FX(3), Y(M3), FX(4), Y(M4))
      G3=H(I, K)
      GA=1. -G2*SL(I, K)
      GB=-(G1+G3)/2. *SL(I, K)
      DO 10 L=1, 4
10 FGP1(K, L)=F(L)
      DO 12 L=1, 4

```

```

12 FGP2(K,L)=F(L)*GA+FX(L)*GB
DO 18 K1=1,4
DO 18 K2=1,4
DO 15 K=1,NGP
13 FGP(K)=FGP1(K,K1)*FGP2(K,K2)
CALL SGINT(FGP,NGP,W,I,IE,FINT)
A(I,K1,K2)=FINT
18 CONTINUE
20 CONTINUE
RETURN
END
SUBROUTINE SCBMY(NT,IE,XG,XGL,XGL2,XGL3,BM,U,Y,H,NGP,W,EL,NTP3,SL)
C
DIMENSION XG(15,5),XGL(15,5),XGL2(15,5),XGL3(15,5),SL(15,5),
1 BM(35),U(32),Y(32),H(15,5),W(15,5),F(4),FX(4),FGP1(5,4),FGP(5)
2 ,EL(15)
DO 10 N=1,NTP3
10 BM(N)=0.
DO 80 I=1,IE
K1=2*I-1
K2=K1+1
K3=K2+1
K4=K3+1
DO 20 IJ=1,NGP
X=XG(I,IJ)
XL=XGL(I,IJ)
XL2=XGL2(I,IJ)
XL3=XGL3(I,IJ)
CALL SFN(X,XL,XL2,XL3,EL,I,F,IE)
CALL SFXN(XL,XL2,EL,I,FX,IE)
G1=TP(F(1),U(K1),F(2),U(K2),F(3),U(K3),F(4),U(K4))
G2=TP(FX(1),U(K1),FX(2),U(K2),FX(3),U(K3),FX(4),U(K4))
G3=TP(F(1),Y(K1),F(2),Y(K2),F(3),Y(K3),F(4),Y(K4))
G4=TP(FX(1),Y(K1),FX(2),Y(K2),FX(3),Y(K3),FX(4),Y(K4))
G5=H(I,IJ)
G6=SL(I,IJ)
AZ=G1*(G4+G6)+(G3+G5)*G2
DO 20 KJ=1,4
20 FGP1(IJ,KJ)=F(KJ)*AZ
KK=K1-1
DO 25 KJ=1,4
K=KK+KJ
DO 22 IJ=1,NGP
22 FGP(IJ)=FGP1(IJ,KJ)
CALL SGINT(FGP,NGP,W,I,IE,FINT)
25 BM(K)=BM(K)-FINT
80 CONTINUE
RETURN
END
SUBROUTINE SCBMU(NT,IE,XG,XGL,XGL2,XGL3,BM,U,Y,H,NGP,W,EL,NTP3,
1 FRICSG,C,SECAL,SINAL,COSAL,COEF,SL)
C
DIMENSION XG(15,5),XGL(15,5),XGL2(15,5),XGL3(15,5),SL(15,5),
1 BM(35),U(32),Y(32),H(15,5),W(15,5),F(4),FX(4),FGP1(5,4),FGP(5),
2 EL(15),PXX(4),SECAL(15),SINAL(15),COSAL(15)
DO 10 N=1,NTP3
10 BM(N)=0.
DO 80 I=1,IE
K1=2*I-1
K2=K1+1
K3=K2+1
K4=K3+1
AMASS=EL(I)*(Y(K1)+Y(K3)+H(I,1)+H(I,5))*0.5
UM=(U(K1)+U(K3))*0.5*SECAL(I)
FD1=COEF*EL(I)*SECAL(I)*UM*ABS(UM)*0.5
FD=FD1/AMASS
DO 20 IJ=1,NGP
DHDX=SL(I,IJ)
X=XG(I,IJ)
XL=XGL(I,IJ)
XL2=XGL2(I,IJ)
XL3=XGL3(I,IJ)
CALL SFN(X,XL,XL2,XL3,EL,I,F,IE)
CALL SFXN(XL,XL2,EL,I,FX,IE)
CALL SFXX(X,EL,I,PXX,IE)
G1=TP(F(1),U(K1),F(2),U(K2),F(3),U(K3),F(4),U(K4))
G2=TP(FX(1),U(K1),FX(2),U(K2),FX(3),U(K3),FX(4),U(K4))
G3=TP(F(1),Y(K1),F(2),Y(K2),F(3),Y(K3),F(4),Y(K4))
G4=TP(FX(1),Y(K1),FX(2),Y(K2),FX(3),Y(K3),FX(4),Y(K4))

```

```

G5=H(I, IJ)
G6=TP(PXX(1), U(K1), PXX(2), U(K2), PXX(3), U(K3), PXX(4), U(K4))
G7=(G3+G5)/2
AZ1=G1*G2+G*G4
AZ2=G1*(G7*DHDX*G6+G4*G2*DHDX)+DHDX*G2*G2+G7
AZ3=FD*(SINAL(I)*G4+COSAL(I))
AZ=AZ1-AZ2+AZ3
DO 20 KJ=1, 4
20 FGP1(IJ, KJ)=F(KJ)*AZ
KK=K1-1
DO 25 KJ=1, 4
K=KK+KJ
DO 22 IJ=1, NOP
22 FGP(IJ)=FGP1(IJ, KJ)
CALL SQINT(FGP, NCP, W, I, IE, FINT)
25 BM(K)=BM(K)-FINT
80 CONTINUE
RETURN
END
SUBROUTINE SQXL(XG, EL, IE, NOP, XGL, XGL2, XGL3, I)
C
DIMENSION XG(15, 5), XGL(15, 5), XGL2(15, 5), XGL3(15, 5), EL(15)
DO 10 K=1, NOP
XGL(I, K)=XG(I, K)/EL(I)
XGL2(I, K)=XGL(I, K)*XGL(I, K)
XGL3(I, K)=XGL2(I, K)*XGL(I, K)
10 CONTINUE
RETURN
END
SUBROUTINE SQINT(FGP, NCP, W, L, IE, FINT)
C
DIMENSION FGP(5), W(15, 5)
FINT=0.
DO 10 I=1, NOP
10 FINT=FINT+FGP(I)*W(L, I)
RETURN
END
SUBROUTINE SPINT(XG, XGL, XGL2, XGL3, IE, EL, W, NCP, I)
C
DIMENSION XG(15, 5), XGL(15, 5), XGL2(15, 5), XGL3(15, 5), W(15, 5), EL(15)
AX=0.5*EL(I)
BX=EL(I)
C
CX=0.538469*AX
BX=0.538469*AX
DX=0.906180*AX
XG(I, 1)=AX-DX
XG(I, 2)=AX-CX
XG(I, 3)=AX
XG(I, 4)=AX+CX
XG(I, 5)=AX+DX
W(I, 1)=0.236927*BX/2.
W(I, 2)=0.478629*BX/2.
W(I, 3)=0.568889*BX/2.
W(I, 4)=W(I, 2)
W(I, 5)=W(I, 1)
RETURN
END
SUBROUTINE SHSL(H, SL, XG, I, XT)
C
DIMENSION H(15, 5), SL(15, 5), XG(15, 5), XT(16)
COMMON /DISTC/ DO, D1, D2, D3
DO 100 J=1, 5
X=XT(I)+XG(I, J)
X2=X*X
X3=X2*X
H(I, J)=DO+D1*X+D2*X2+D3*X3
100 SL(I, J)=D1+2.*D2*X+3.*D3*X2
RETURN
END
FUNCTION TP(A, B, C, D, E, F, G, H)
TP=A*B+C*D+E*F+G*H
RETURN
END
SUBROUTINE BANDS1(N, NHB, NHBP1, NHBM1, NFB, A, B, VARC, C, NTP3)
C
DIMENSION A(32, 7), B(35), VAR(35), VARC(25), COR(35), C(32, 7), R(35)
DO 40 I=1, N
40 R(I)=B(I)
DO 50 I=1, NTP3
VAR(I)=0.

```



```

50  VARC(I)=0.
60  DO 300 I=2,N
    IM1=I-1
    KE=NHB
    DO 100 L=1,NHBM1
100  IF(I.EQ.(N-L+1)) KE=L
    DO 300 K=1,KE
    JBM1=NHBP1-K
    IK1=I+K-1
    B(IK1)=B(IK1)-B(IM1)*A(IK1,JBM1)
300  CONTINUE
    DO 500 J=1,N
    I=N-J+1
    S=0.
    DO 400 M=1,NHB
400  S=S+VAR(I+M)*A(I,NHB+M+1)
    VAR(I)=(B(I)-S)/A(I,NHBP1)
500  CONTINUE
    DO 520 I=1,N
    CDR(I)=VAR(I)
520  VARC(I)=VARC(I)+VAR(I)
    DO 540 I=1,N
    IF(ABS(CDR(I)/VARC(I)-1.).GE.0.1) GO TO 560
540  CONTINUE
    GO TO 800
560  S=C(1,4)*VARC(1)+C(1,5)*VARC(2)+C(1,6)*VARC(3)+C(1,7)*VARC(4)
    B(1)=R(1)-S
    S=C(2,3)*VARC(1)+C(2,4)*VARC(2)+C(2,5)*VARC(3)+C(2,6)*VARC(4)+
    1 C(2,7)*VARC(5)
    B(2)=R(2)-S
    S=C(3,2)*VARC(1)+C(3,3)*VARC(2)+C(3,4)*VARC(3)+C(3,5)*VARC(4)+
    1 C(3,6)*VARC(5)+C(3,7)*VARC(6)
    B(3)=R(3)-S
    DO 700 I=4,N
    KB=I-3
    S=0.
    DO 600 J=1,7
    K=KB+J-1
600  S=S+C(I,J)*VARC(K)
700  B(I)=R(I)-S
    GO TO 60
800  RETURN
    END

```

SUBROUTINE SPBAND(N,NHB,NHBP1,NHBM1,NFB,A,IB,IEND)

```

C
    DIMENSION A(32,7)
    DO 300 I=IB,IEND
    IM1=I-1
    KE=NHB
    DO 100 L=1,NHBM1
100  IF(I.EQ.(N-L+1))KE=L
    DO 300 K=1,KE
    JBM1=NHBP1-K
    JB=JBM1+1
    IK1=I+K-1
    IF(A(IK1,JBM1).EQ.0.) GO TO 300
    KK=NFB-K
    F=A(IK1,JBM1)/A(IM1,NHBP1)
    A(IK1,JBM1)=F
    DO 200 J=JB,KB
200  A(IK1,J)=A(IK1,J)-A(IM1,J+K)*F
300  CONTINUE
    RETURN
    END
    SUBROUTINE REST1S(CC,CY,IN,IM)

```

```

C
    DIMENSION CC(2,3),CY(32,7)
    K=0
    DO 10 I=IN,IM
    K=K+1
    DO 10 J=1,3
10  CC(K,J)=CY(I,J)
    RETURN
    END
    SUBROUTINE REST2S(CC,CY,IN,IM)

```

```

C
    DIMENSION CC(2,3),CY(32,7)
    K=0
    DO 10 I=IN,IM

```

```

K=K+1
DO 10 J=1,3
10 CY(I,J)=CC(K,J)
RETURN
END
SUBROUTINE SCREW(IND, U, Y, H, EL, IE, NT, NTM1, NTM2, NTM3, NTM5, CC, UL,
1 NTP3, SL, NCP, W, A, AB, CY, UD, ED, NFB, XG, XGL, XGL2, XGL3, CCY, XT)
C
DIMENSION U(32), Y(32), H(15,5), EL(15), W(15,5), A(15,4,4), SL(15,5),
1 AB(4,4), CY(32,7), UD(35), ED(35), AB(4,4), F(4), XT(15),
2 XG(15,5), XGL(15,5), XGL2(15,5), XGL3(15,5), CC(2,3), CCY(32,7)
COMMON /DISTC/ DO, D1, D2, D3
IND=1
UOLD=U(NTM1)
UDOLD=UD(NTM1)
YOLD=Y(NTM1)
EDOLD=ED(NTM1)
UPOLD=U(NT)
UDPOLD=UD(NT)
YPOLD=Y(NT)
EDPOLD=ED(NT)
ELOLD=EL(IE)
UM2=U(NTM3)
UP2=U(NTM2)
YM2=Y(NTM3)
YP2=Y(NTM2)
UDM2=UD(NTM3)
UDP2=UD(NTM2)
EDM2=ED(NTM3)
EDP2=ED(NTM2)
IEM1=IE
IE=IE+1
NT=NT+2
NTM1=NT-1
NTM2=NT-2
NTM3=NT-3
NTM4=NT-4
NTM5=NT-5
NTM6=NT-6
NTM7=NT-7
NTP1=NT+1
NTP3=NT+3
U(NT)=UPOLD
Y(NT)=YPOLD
U(NTM1)=UOLD
Y(NTM1)=YOLD
EL(IEM1)=0.8*UL
XT(IE)=XT(IEM1)+EL(IEM1)
EL(IE)=ELOLD-EL(IEM1)
X=EL(IEM1)
XL=X/ELOLD
XL2=XL*XL
XL3=XL2*XL
F1=1.-3.*XL2+2.*XL3
F2=X+ELOLD*(XL3-2.*XL2)
F3=3.*XL2-2.*XL3
F4=ELOLD*(XL3-XL2)
FX1=6.*(XL2-XL)/ELOLD
FX2=1.-4.*XL+3.*XL2
FX3=6.*(XL-XL2)/ELOLD
FX4=3.*XL2-2.*XL
U(NTM3)=F1*UM2+F2*UP2+F3*UOLD+F4*UPOLD
U(NTM2)=F1*UM2+FX2*UP2+FX3*UOLD+FX4*UPOLD
UD(NTM3)=F1*UDM2+F2*UDP2+F3*UDOLD+F4*UDPOLD
UD(NTM2)=F1*UDM2+FX2*UDP2+FX3*UDOLD+FX4*UDPOLD
DO 20 II=NTP1, NTP3
UD(II)=0.
ED(II)=0.
20 Y(NTM3)=F1*YM2+F2*YP2+F3*YOLD+F4*YPOLD
Y(NTM2)=F1*YM2+FX2*YP2+FX3*YOLD+FX4*YPOLD
ED(NTM3)=F1*EDM2+F2*EDP2+F3*EDOLD+F4*EDPOLD
ED(NTM2)=F1*EDM2+FX2*EDP2+FX3*EDOLD+F4*EDPOLD
DO 32 I=IEM1, IE
CALL SPINT(XG, XGL, XGL2, XGL3, IE, EL, W, NCP, I)
CALL SCXL(XG, EL, IE, NCP, XGL, XGL2, XGL3, I)
CALL SHSL(H, SL, XG, I, XT)
32 CONTINUE
CALL CELCS(A, F, NCP, W, XG, XGL, XGL2, XGL3, EL, IE, IEM1)
DO 38 J1=1,2
DO 38 J2=1,2

```

```

38 AB1(J1, J2)=A(IEM1, J1+2, J2+2)
   DO 25 J1=1, 2
   DO 25 J2=1, 2
25 A(IEM1, J1, J2)=A(IEM1, J1, J2)+AB(J1, J2)
   CALL REST25(CC, CY, NTM5, NTM4)
   K1=2+IEM1-1
   K4=K1+3
   M1=0
   DO 75 N1=K1, K4
   M1=M1+1
   LL=4-M1
   DO 75 N2=1, 4
   L=LL+N2
   CY(N1, L)=A(IEM1, M1, N2)
75 CCY(N1, L)=CY(N1, L)
   CALL REST15(CC, CY, NTM3, NTM2)
   DO 28 J1=1, 2
   DO 28 J2=1, 2
28 AB(J1, J2)=AB1(J1, J2)
   RETURN
   END
SUBROUTINE GDIST(A, B, C, D, DIST1, DIST)
C
   N=0
   DWN=100.
   WN=DIST1-100.
5   N=N+1
   WN=WN+DWN
   GRR=A*WN**3+B*WN**2+C*WN+D
   IF(N-1) 20, 20, 25
20  T1=GRR
   GO TO 5
25  IF(ABS(GRR), LT, 0.01) GO TO 1000
   IF((T1/GRR), LT, 0.0) GO TO 1020
   IF((T1/GRR), LT, 1.0) GO TO 1010
   T1=GRR
   GO TO 5
1000 DIST=WN
   GO TO 30
1010 DWN=-DWN
   T1=GRR
   GO TO 5
1020 WN=WN-DWN
   DWN=DWN/2.
   GO TO 5
30  RETURN
   END

```